

Joint Transceiver Design Algorithms for Multiuser MISO Relay Systems with Energy Harvesting

Yunlong Cai, Ming-Min Zhao, Qingjiang Shi, Benoit Champagne and Min-Jian Zhao

Abstract—In this paper, we investigate a multiuser multiple-input single-output (MISO) relay system with simultaneous wireless information and power transfer (SWIPT), where the received signal is divided into two parts for information decoding (ID) and energy harvesting (EH), respectively. Assuming that both base station (BS) and relay station (RS) are equipped with multiple antennas, this work studies the joint transceiver design problem for the BS beamforming vectors, the RS amplify-and-forward (AF) transformation matrix and the power splitting (PS) ratios at the single-antenna receivers. The aim is to minimize the total transmission power of the BS and the RS under both signal-to-interference-plus-noise ratio (SINR) and EH constraints. Firstly, an iterative algorithm based on alternating optimization (AO) and with guaranteed convergence is proposed to successively optimize the transceiver coefficients. This AO-based approach is then extended into a robust transceiver design against quantization errors in channel state information (CSI), by using semidefinite relaxation (SDR) and the S-procedure. Secondly, a novel design scheme based on switched relaying (SR) is proposed that can significantly reduce the computational complexity and overhead of the AO-based designs while maintaining a similar performance. In the proposed SR scheme, the RS is equipped with a codebook of permutation matrices. For each permutation matrix, a latent transceiver is designed which consists of BS beamforming vectors, optimally scaled RS permutation matrix and receiver PS ratios. For the given CSI, the optimal transceiver with the lowest total power consumption is selected for transmission. We propose a concave-convex procedure (CCCP) based and subgradient-type iterative algorithms for the non-robust and robust latent transceiver designs. Simulation results are presented to validate the effectiveness of all the proposed algorithms.

Index Terms—Beamforming, concave-convex procedure, switched relaying, power splitting, energy harvesting, SWIPT.

I. INTRODUCTION

Recently, electromagnetic (EM) energy transfer techniques have attracted considerable interest in the wireless research community. Indeed, by exploiting the radiative far-field properties of EM waves, these techniques could in theory enable a radio receiver to harvest energy from its environment, thereby

relaxing the battery requirements on user devices. An interesting application of wireless energy transfer is to jointly transmit information and energy using the same waveform, which is known as simultaneous wireless information and power transfer (SWIPT). The idea of SWIPT was first proposed by Varshney in [1], which characterizes the rate-energy (R-E) tradeoff in a discrete memoryless channel. The study of the R-E tradeoff was later extended to frequency selective fading channels in [2]. In [3], the authors studied a two-way communication scenario with noiseless channels and limited resources, with emphasis on the tradeoffs due to the need of balancing the information flow with the resulting energy exchange among the communicating nodes. The authors of [4] focused on multiuser systems and demonstrated that energy transfer constraints call for additional coordination among distributed nodes of a wireless network. However, the above studies have not been realized yet due to practical circuit limitations.

The first practical receiver structure that makes SWIPT possible was proposed in [5], where two practical signal separation schemes were considered, namely, the time switching (TS) scheme, where the receiver switches between information decoding (ID) and energy harvesting (EH), and the power splitting (PS) scheme, where the received signal is split into two streams, such that a fraction ρ ($0 \leq \rho \leq 1$) of the received signal power is used for ID while the remaining fraction $(1-\rho)$ is used for EH. PS-based algorithms were considered in [6]–[10]. In [6], the authors derived the optimal PS rule at the receiver, for both SISO (single-input single-output) and SIMO (single-input multiple-output) systems, in order to optimize the R-E performance tradeoff. In [7], the authors proposed two practical receiver architectures, i.e., separated and integrated information and energy receivers, based on dynamic power splitting. These authors characterized the R-E performance by taking circuit power consumption into account.

The authors of [8] studied the joint beamforming and power splitting (JBPS) design for a multiuser multiple-input single-output (MISO) broadcast system with SWIPT. In this study, the total transmission power at the base station (BS) is minimized subject to signal-to-interference-plus-noise ratio (SINR) and EH constraints for all the receivers. The JBPS problem for a K -user MISO interference channel was considered in [9], where the authors used the semidefinite relaxation (SDR) technique to address the non-convex problem and proved that the SDR is tight in the case of $K = 2$ or 3 . Different from the approach of [9], an alternative second-order-cone-programming (SOCP) relaxation method was proposed in [10]. The SOCP relaxation based method guarantees a feasible so-

Y. Cai, M. M. Zhao and M. J. Zhao are with the College of Information Science and Electronic Engineering, Zhejiang University, Hangzhou 310027, China (e-mail: ylcai@zju.edu.cn; zmblack@zju.edu.cn; mjzhao@zju.edu.cn).

Q. Shi is with the School of Info. Sci. & Tech., Zhejiang Sci-Tech University, Hangzhou 310018, China. He is also with The State Key Laboratory of Integrated Services Networks, Xidian University (email: qing.j.shi@gmail.com).

B. Champagne is with the Department of Electrical and Computer Engineering, McGill University, Montreal, QC H3A 0E9, Canada (benoit.champagne@mcgill.ca).

This work was supported in part by the National Natural Science Foundation of China under Grant 61471319, Zhejiang Provincial Natural Science Foundation of China under Grant LY14F010013, the Fundamental Research Funds for the Central Universities, and the National High Technology Research and Development Program (863 Program) of China under Grant 2014AA01A707.

lution to the JBPS problem and has lower complexity than the SDR method, while achieving a performance extremely close to the minimum transmission power. A primal-decomposition based decentralized algorithm was also presented in this work.

Besides, the SWIPT technique for relay systems was considered in [11]–[14]. Specifically, the authors of [11] proposed a joint source and relay precoding design algorithm to achieve different tradeoffs between the energy transfer and the information rate. In [12], the relay beamforming design problem for the SWIPT scheme was considered in a non-regenerative two-way multi-antenna relay network, where a global optimal solution, a local optimal solution and a low-complexity suboptimal solution were proposed. The design of a high-rate beamformer that supports multiple communication pairs and intended for SWIPT in wireless relay networks was considered in [13]. In [14], a game-theoretical framework was developed to address the distributed power splitting problem for SWIPT in relay interference channels. The aforementioned works assume the availability of perfect channel state information (CSI), which may be impractical in realistic implementations of these systems.

In this paper, we consider the use of PS-based receivers in a general multiuser MISO relay systems, i.e., where a multi-antenna relay station (RS) is incorporated into the traditional MISO multiuser setup, as in [15]–[17]. We focus our study on the downlink transmission where the BS first transmits the signals intended for different receivers via beamforming to the RS. Then, the RS processes the received signals through an amplify-and-forward (AF) transformation matrix and broadcasts it to all the receivers. Finally, each receiver employs the PS technique to decode information and harvest energy simultaneously. We present an optimization framework for the joint design of the BS beamforming vectors, the RS AF transformation matrix and the receiver PS ratios aiming to minimize the total power consumption under a set of minimum SINR and EH constraints at the receivers. In this work, we shall assume that the proposed joint design algorithms are implemented at the BS.¹

To this end, we first propose an iterative algorithm based on alternating optimization (AO) and with guaranteed convergence to successively optimize the transceiver coefficients, i.e. the BS beamformers, the AF transformation matrix and the receiver PS ratios. We show that each subproblem can be relaxed as a semidefinite programming (SDP) problem by applying the celebrated SDR technique [21]. This AO-based approach is then extended into a robust transceiver design against quantization errors in CSI based on the SDR technique and the S-procedure [22], [23]. While the performance of the AO-based designs is remarkable, we note that in this approach, the BS needs to compute and send the complete AF matrix to the RS before transmission, which entails high design complexity and signaling requirements for the overhead. Secondly, to reduce the design and implementation costs, we present extensions of the switched relaying (SR)

processing reported in [24] to multiuser MISO relay systems with energy harvesting. For this scheme, we equip the RS with a codebook of permutation matrices. Based on each element of the codebook, we can obtain a permuted channel matrix and therefore create a latent transceiver, which includes the BS beamforming vectors, an optimally scaled relaying permutation matrix and the receiver PS ratios. Among the latent transceivers so obtained for given CSI, the optimal one is chosen according to a suitable criterion for transmission.

Specifically, SR-based algorithm constructs the RS AF transformation matrix within each latent transceiver by multiplying a permutation matrix from the codebook with a power scaling factor. Before data transmission, the BS sends the index of the permutation matrix (instead of the RS AF transformation matrix), the RS power scaling factor, and the PS ratios corresponding to the optimal transceiver to the RS and the receivers through signaling channels. Compared to the AO-based algorithms, the SR approach reduces the number of optimization variables from the complete RS AF transformation matrix to a single power scaling factor, which in turn significantly reduces the computational complexity and signaling overhead. To design the latent transceivers in the SR scheme, an iterative algorithm based on the concave-convex procedure (CCCP) [25], [26] is proposed that uses the estimated CSI, and is guaranteed to converge to a local optimal point. Each subproblem in the iterative algorithm can be formulated as an SOCP problem. By taking the quantization CSI errors into account, we propose a robust subgradient algorithm which utilizes the side information provided by standard convex solvers. Furthermore, a simplified SR-based transceiver design algorithm is proposed with much less computational complexity, while achieving a performance extremely close to the non-simplified scheme. Finally, two efficient codebook design approaches are developed.

Simulation results demonstrate that the proposed transceiver design algorithms are capable of providing robustness against the effects of norm-bounded CSI errors. In particular, the SR-based algorithms using a small codebook of permutation matrices can achieve almost the same performance as the AO-based algorithms but with reduced design/implementation complexity and signaling overhead.

The remainder of this paper is organized as follows. Section II presents the multiuser MISO relay system model, the channel error model and the problem formulation. In Section III, the AO-based transceiver design algorithms for both non-robust and robust cases are developed. Section IV discusses the SR-based transceiver scheme, including the proposed latent transceiver design algorithms and the codebook design methods. A complexity analysis of the proposed algorithms along with a discussion of their initialization are provided in Section V. Finally, in Section VI computer simulations are used to verify the proposed algorithms. Conclusions are drawn in Section VII.

Notations: Scalars, vectors and matrices are respectively denoted by lower case, boldface lower case and boldface upper case letters. For a square matrix \mathbf{A} , $\text{Tr}(\mathbf{A})$, $\text{rank}(\mathbf{A})$, \mathbf{A}^T , $\text{conj}(\mathbf{A})$, and \mathbf{A}^H denote its trace, rank, transpose, conjugate, and conjugate transpose respectively, while $\mathbf{A} \succeq \mathbf{0}$ means that

¹In practice, in cellular systems it is preferable to implement most of the signal processing operations at the BS rather than the RS due to the fact that the BS is more powerful and the RS is expected to have a simple structure and low energy consumption [18]–[20].

\mathbf{A} is a positive semidefinite matrix. The operator $\text{vec}(\cdot)$ stacks the elements of a matrix in one long column vector, $\text{invp}(x)$ denotes the inverse of the positive portion, i.e., $\frac{1}{\max(x,0)} \cdot \|\cdot\|$, $(\cdot)!$, and $|\cdot|$ denote the Euclidean norm of a complex vector, the factorial operator, and the absolute value of a complex scalar, respectively. $\mathbb{C}^{m \times n}$ ($\mathbb{R}^{m \times n}$) denotes the space of $m \times n$ complex (real) matrices, and \mathbb{R}_+ (\mathbb{R}_-) denotes the set of positive (negative) real numbers. Finally, the symbol \otimes denotes the Kronecker product of two vectors/matrices.

II. SYSTEM MODEL AND PROBLEM FORMULATION

A. Proposed System Model

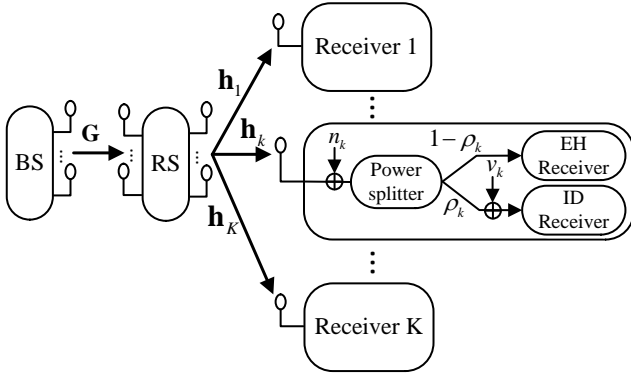


Fig. 1. The multiuser MISO relay system with PS-based receiver. Each receiver splits the received signal into two parts for ID and EH, respectively.

In this work, we consider a multiuser MISO relay system which consists of one BS, one RS, and K mobile receivers indexed by $k \in \mathcal{K} \triangleq \{1, \dots, K\}$. The number of antennas at the BS and the RS is denoted as N_t and N_r , respectively, while each receiver is equipped with a single antenna. We assume that $K \leq \min\{N_t, N_r\}$, which provides sufficient degrees of freedom for signal detection. We also assume that the classical two-hop AF relaying protocol [27] is employed, and that the direct links between the BS and the receivers are sufficiently weak (to be ignored). Different from the conventional multiuser MISO relay channels [17], we here consider PS-based receivers. The received signal at each receiver is split into two separate signal streams with different power levels: one is sent to the EH receiver and the other one is diverted to the ID receiver [5], as shown in Fig. 1. Under the above assumptions, the signals are transmitted in two phases as explained below.

In the first phase, the BS transmits K data streams, each carrying an independent message intended for one of the K receivers. Thus, the transmitted data vector at the BS can be expressed as

$$\mathbf{x}_B = \sum_{k=1}^K \mathbf{f}_k s_k, \quad (1)$$

where s_k is the data signal for receiver k , with zero mean and variance $E\{|s_k|^2\} = 1$, and $\mathbf{f}_k \in \mathbb{C}^{N_t \times 1}$ denotes the transmit beamforming vector. The data signals $\{s_k\}_{k \in \mathcal{K}}$ are assumed to be independent of each other. The transmit power of the

BS can be shown as

$$P_B = E\{\mathbf{x}_B \mathbf{x}_B^H\} = \sum_{k=1}^K \|\mathbf{f}_k\|^2. \quad (2)$$

The transmission from the BS to the RS can be modeled as a standard point-to-point MIMO channel. Hence, the received data vector at the RS can be expressed as

$$\mathbf{y}_R = \mathbf{G} \sum_{k=1}^K \mathbf{f}_k s_k + \mathbf{n}_r, \quad (3)$$

where $\mathbf{G} \in \mathbb{C}^{N_r \times N_t}$ denotes the MIMO channel from the BS to the RS, and $\mathbf{n}_r \in \mathbb{C}^{N_r \times 1}$ is the complex circular Gaussian noise vector at the RS, with zero mean and covariance $E\{\mathbf{n}_r \mathbf{n}_r^H\} = \sigma_r^2 \mathbf{I}$, where σ_r^2 is the average noise power. It is assumed that the transmitted signals $\{s_k\}_{k \in \mathcal{K}}$ are independent of the noise vector \mathbf{n}_r .

In the second phase, the RS forwards the received signal to all the receivers after performing linear AF processing. Hence the vector signal transmitted from the RS can be formulated as

$$\mathbf{x}_R = \mathbf{W} \mathbf{y}_R, \quad (4)$$

where $\mathbf{W} \in \mathbb{C}^{N_r \times N_r}$ is the AF transformation matrix at the RS. The transmission power of the RS can be shown as

$$P_R = E\{\mathbf{x}_R \mathbf{x}_R^H\} = \sum_{k=1}^K \|\mathbf{W} \mathbf{G} \mathbf{f}_k\|^2 + \sigma_r^2 \|\mathbf{W}\|^2. \quad (5)$$

Finally, The signal received at the k th receiver, $k \in \mathcal{K}$, is given by

$$y_k = \mathbf{h}_k^H \mathbf{W} \mathbf{G} \sum_{k=1}^K \mathbf{f}_k s_k + \mathbf{h}_k^H \mathbf{W} \mathbf{n}_r + n_k, \quad (6)$$

where $\mathbf{h}_k \in \mathbb{C}^{N_r \times 1}$ denotes the complex conjugate channel vector between the RS and receiver k , and n_k is the additive noise introduced by the receive antenna at receiver k , which is assumed to be a complex circular Gaussian variable with zero mean and variance σ_k^2 .

Let ρ_k ($0 \leq \rho_k \leq 1$) denotes the PS ratio for receiver k , which means that portion ρ_k of the signal power is used for signal detection while the remaining portion $1 - \rho_k$ is diverted to an energy harvester. Thus, on the one hand, the signal available for ID at receiver k can be expressed as

$$\mathbf{r}_k^{\text{ID}} = \sqrt{\rho_k} \left(\mathbf{h}_k^H \mathbf{W} \mathbf{G} \sum_{k=1}^K \mathbf{f}_k s_k + \mathbf{h}_k^H \mathbf{W} \mathbf{n}_r + n_k \right) + v_k, \quad (7)$$

where v_k is the additional complex circular Gaussian circuit noise with zero mean and variance $E\{|v_k|^2\} = \omega_k^2$, resulting from phase offsets and non-linearities during baseband conversion [5]. Thus, the SINR at the k th receiver can be expressed as

$$\Gamma_k = \frac{\rho_k |\mathbf{h}_k^H \mathbf{W} \mathbf{G} \mathbf{f}_k|^2}{\rho_k \left(\sum_{j \neq k} |\mathbf{h}_k^H \mathbf{W} \mathbf{G} \mathbf{f}_j|^2 + \sigma_r^2 \|\mathbf{h}_k^H \mathbf{W}\|^2 + \sigma_k^2 \right) + \omega_k^2}. \quad (8)$$

On the other hand, the total harvested energy that can be stored by receiver k is equal to

$$P_k^{\text{EH}} = \xi_k(1 - \rho_k) \left(\sum_{j=1}^K |\mathbf{h}_k^H \mathbf{W} \mathbf{G} \mathbf{f}_j|^2 + \sigma_r^2 \|\mathbf{h}_k^H \mathbf{W}\|^2 + \sigma_k^2 \right), \quad (9)$$

where $\xi_k \in (0, 1]$ denotes the energy conversion efficiency of the k th EH unit, which indicates that only a portion ξ_k of the radio frequency energy can be stored.

B. Channel Error Model

We assume that the required CSI can be estimated at the BS and the RS by means of a suitable channel estimation algorithms [28]–[30]. In this work, we consider a time division duplex (TDD) mode and assume that the radio channels vary sufficiently slowly over time, so that the downlink transmit CSI can be obtained by channel reciprocity [31]. Therefore, the BS can obtain the MIMO channel matrix \mathbf{G} involved the first phase of transmission, while the RS can obtain the channel vectors $\{\mathbf{h}_k\}$ involved in the second. However, the second phase CSI needs to be fed back from the RS to the BS using signaling channels [31]–[33] for implementation of the design algorithms, as explained earlier. Hence, here we assume that the BS can perfectly know the first phase CSI, matrix \mathbf{G} , but not the second phase CSI, i.e. vectors $\{\mathbf{h}_k\}$. We consider quantization errors during channel feedback from the RS to the BS and employ the NBE model [34] to characterize this type of imperfection. In particular, the true (but unknown) second phase CSI can be expressed as follows:

$$\mathbf{h}_k = \hat{\mathbf{h}}_k + \mathbf{e}_k, \quad k \in \mathcal{K}, \quad (10)$$

where $\hat{\mathbf{h}}_k$ denotes the estimated channel vector, while \mathbf{e}_k denotes the CSI error vector. We assume that vector \mathbf{e}_k is bounded in its Euclidean norm, that is

$$\|\mathbf{e}_k\| \leq \eta_k, \quad k \in \mathcal{K}, \quad (11)$$

where η_k is a known positive constant. Equivalently, \mathbf{h}_k belongs to the uncertainty set \mathfrak{R}_k defined as

$$\mathfrak{R}_k = \{\mathbf{h} | \mathbf{h} = \hat{\mathbf{h}}_k + \mathbf{e}_k, \|\mathbf{e}_k\| \leq \eta_k\}, \quad k \in \mathcal{K}. \quad (12)$$

The shape and the size of \mathfrak{R}_k model the type of uncertainty in the estimated CSI, which is linked to the physical phenomenon producing the CSI errors. It should be emphasized that the actual errors \mathbf{e}_k are assumed to be unknown while the corresponding upper bounds η_k can be obtained using preliminary knowledge about the type of imperfection and/or coarse knowledge of the channel type and main characteristics [35].

C. Problem Formulation

In this subsection, we formulate the optimization problem for the joint design of \mathbf{W} , $\{\mathbf{f}_k\}_{k \in \mathcal{K}}$ and $\{\rho_k\}_{k \in \mathcal{K}}$ so as to minimize the total power consumption at the BS and the RS under the constraint that a set of minimum SINR and EH targets be

satisfied at the receivers. In this study, we consider both non-robust and robust designs (against quantization errors).² The non-robust optimization problem can be expressed as³

$$\begin{aligned} & \min_{\mathbf{W}, \{\mathbf{f}_k, \rho_k\}} P_B + P_R \\ & \text{s.t. } \Gamma_k \geq \gamma_k, P_k^{\text{EH}} \geq \psi_k, \\ & 0 \leq \rho_k \leq 1, \forall k \in \mathcal{K}, \end{aligned} \quad (13)$$

where in the evaluation of (8) and (9), the true channel vectors \mathbf{h}_k are replaced by their estimates $\hat{\mathbf{h}}_k$.

Similarly, the robust optimization problem can be formulated as

$$\begin{aligned} & \min_{\mathbf{W}, \{\mathbf{f}_k, \rho_k\}} P_B + P_R \\ & \text{s.t. } \Gamma_k \geq \gamma_k, P_k^{\text{EH}} \geq \psi_k, \\ & 0 \leq \rho_k \leq 1, \|\mathbf{e}_k\|^2 \leq \eta_k^2, \forall k \in \mathcal{K}, \end{aligned} \quad (14)$$

where in this case, the channel vectors in (8) and (9) are given by (10).

It is not difficult to see that both (13) and (14) are in general non-convex because both their objective functions and constraints are not convex over \mathbf{W} , $\{\mathbf{f}_k\}$ and $\{\rho_k\}$. Furthermore, (14) involves an infinite number of constraints. These characteristics make it intractable to obtain the global optimal solution for (13) and (14). In the sequel, we present two algorithms for obtaining suboptimal solutions to the above problems by applying proper convex optimization techniques, which are based on AO and SR, respectively. We complete this section with the following lemma.

Lemma 1: Problem (13) is feasible for any finite user SINR targets if $\text{rank}(\mathbf{H}\mathbf{G}) = K$, where $\mathbf{H} = [\mathbf{h}_1, \dots, \mathbf{h}_K]^H$.

Proof: The feasibility of (13) is not connected to the EH constraints and PS ratios according to Lemma 3.1 & Lemma 3.2 in [36]. Hence, according to *Theorem 1* in [17], we can easily see that the above lemma holds.

On the other hand, the feasibility of problem (14) has not been well studied in the literature and still remains an open question, which would be an interesting topic for future research.

III. ALTERNATING OPTIMIZATION BASED JOINT TRANSCIVER DESIGN

In this section, we present the AO-based transceiver design algorithms for the jointly optimization of the BS beamforming vectors, the RS AF transformation matrix and the receiver PS ratios, for both non-robust and robust cases. In the proposed design, $\{\mathbf{f}_k, \rho_k\}_{k \in \mathcal{K}}$ and \mathbf{W} are successively optimized in turn with the other fixed. We show that each subproblem for the optimization of $\{\mathbf{f}_k, \rho_k\}$ or \mathbf{W} can be reformulated as an SDP problem based on the celebrated SDR technique and the S-procedure. Furthermore, modified randomization techniques based on the worst-case concept are provided to recover a rank-one solution when higher-rank solutions are returned.

²The non-robust joint design is only based on the estimated CSI, while the robust design algorithm takes the CSI error into account.

³There is in general a power consumption tradeoff between the BS and the RS [17], and the objective function should be $P_B + \alpha P_R$ where α is a positive weight. We assume that $\alpha = 1$ in this work, since this does not change the nature of the problem.

A. Non-Robust AO-Based Joint Transceiver Design

In the following, we introduce a non-robust joint transceiver design algorithm. First, let us consider the optimization of $\{\mathbf{f}_k, \rho_k\}$ in (13) while the RS AF matrix \mathbf{W} is fixed. The celebrated SDR technique can be applied to solve the remaining optimization problem by introducing a new variable $\mathbf{F}_k = \mathbf{f}_k \mathbf{f}_k^H$. Hence, problem (13) can be reformulated as the following problem by ignoring the rank-one constraints for all \mathbf{F}_k 's:

$$\begin{aligned} & \min_{\{\mathbf{F}_k, \rho_k\}} \sum_{k=1}^K \text{Tr}(\mathbf{F}_k) + \sum_{k=1}^K \text{Tr}(\mathbf{Q}_k) + \sigma_r^2 \|\mathbf{W}\|^2 \\ & \text{s.t. } \frac{1}{\gamma_k} \hat{\mathbf{h}}_k^H \mathbf{Q}_k \hat{\mathbf{h}}_k - \sum_{j \neq k} \hat{\mathbf{h}}_k^H \mathbf{Q}_j \hat{\mathbf{h}}_k \geq \sigma_r^2 \|\hat{\mathbf{h}}_k^H \mathbf{W}\|^2 + \sigma_k^2 + \frac{\omega_k^2}{\rho_k}, \\ & \sum_{j=1}^K \hat{\mathbf{h}}_k^H \mathbf{Q}_j \hat{\mathbf{h}}_k \geq \frac{\psi_k}{\xi_k(1-\rho_k)} - \sigma_k^2 - \sigma_r^2 \|\hat{\mathbf{h}}_k^H \mathbf{W}\|^2, \\ & \mathbf{F}_k \succeq \mathbf{0}, 0 \leq \rho_k \leq 1, \forall k \in \mathcal{K}, \end{aligned} \quad (15)$$

where $\mathbf{Q}_k = \mathbf{W} \mathbf{G} \mathbf{F}_k \mathbf{G}^H \mathbf{W}^H$. In this way, problem (13) is relaxed to a convex SDP problem, which can be efficiently solved by off-the-shelf algorithms [37]. Let $\{\mathbf{F}_k^*\}$ and $\{\rho_k^*\}$ denote the optimal solution to (15). Based on *Proposition 4.1* in [36], it can be verified that $\{\mathbf{F}_k^*\}$ and $\{\rho_k^*\}$ satisfy the first two sets of constraints of problem (15) with equality and $\{\mathbf{F}_k^*\}$ satisfy $\text{rank}(\mathbf{F}_k^*) = 1, \forall k$. Thus the optimal solution of problem (13) can be expressed as $\{\mathbf{f}_k^*, \rho_k^*\}$, where \mathbf{f}_k^* is the principal component of \mathbf{F}_k^* , such that $\mathbf{F}_k^* = \mathbf{f}_k^* \mathbf{f}_k^{*H}$, $\|\mathbf{f}_k^*\| = \sqrt{f_k}$ and f_k is the largest eigenvalue of \mathbf{F}_k^* .

Next, we consider the optimization of the RS AF matrix \mathbf{W} while assuming that $\{\mathbf{f}_k, \rho_k\}$ are fixed. Noting that $\mathbf{x}^T \mathbf{Y} \mathbf{z} = \text{vec}(\mathbf{x} \mathbf{z}^T)^T \text{vec}(\mathbf{Y})$, the numerator in (8) can be rewritten as

$$\begin{aligned} \rho_k |\hat{\mathbf{h}}_k^H \mathbf{W} \mathbf{G} \mathbf{f}_k|^2 &= \rho_k |\mathbf{g}_{kk}^T \text{vec}(\mathbf{W})|^2 \\ &= \rho_k \mathbf{g}_{kk}^T \widetilde{\mathbf{W}} \text{conj}(\mathbf{g}_{kk}), \end{aligned} \quad (16)$$

where $\mathbf{g}_{kj} = \text{vec}(\text{conj}(\hat{\mathbf{h}}_k) \mathbf{f}_j^T \mathbf{G}^T)$ and $\widetilde{\mathbf{W}} = \text{vec}(\mathbf{W}) \text{vec}(\mathbf{W})^H$. Similarly, the denominator in (8) can be reformulated as

$$\begin{aligned} & \rho_k \sum_{j \neq k} \mathbf{g}_{kj}^T \widetilde{\mathbf{W}} \text{conj}(\mathbf{g}_{kj}) \\ & + \rho_k \sigma_r^2 \sum_{j=1}^{N_r} \hat{\mathbf{h}}_k^H \mathbf{E}_j \widetilde{\mathbf{W}} \mathbf{E}_j^H \hat{\mathbf{h}}_k + \rho_k \sigma_k^2 + \omega_k^2, \end{aligned} \quad (17)$$

where $\mathbf{E}_k \in \{0, 1\}^{N_r \times N_r^2}$ is a linear mapping matrix such that $\hat{\mathbf{h}}_k^H \mathbf{E}_j \text{vec}(\mathbf{W}) = \hat{\mathbf{h}}_k^H \mathbf{W}(:, j)$, where $\mathbf{W}(:, j)$ denotes the j th column of \mathbf{W} . With the help of (16) and (17), the SINR and EH constraints in problem (13) can be expressed as the following two inequalities

$$\frac{1}{\gamma_k} \mathbf{g}_{kk}^T \widetilde{\mathbf{W}} \text{conj}(\mathbf{g}_{kk}) - \sum_{j \neq k} \mathbf{g}_{kj}^T \widetilde{\mathbf{W}} \text{conj}(\mathbf{g}_{kj}) - \sigma_r^2 \sum_{j=1}^{N_r} \hat{\mathbf{h}}_k^H \mathbf{E}_j \widetilde{\mathbf{W}} \mathbf{E}_j^H \hat{\mathbf{h}}_k \geq \sigma_k^2 + \frac{\omega_k^2}{\rho_k}, \quad (18)$$

$$\begin{aligned} & \sum_{j=1}^K \mathbf{g}_{kj}^T \widetilde{\mathbf{W}} \text{conj}(\mathbf{g}_{kj}) + \\ & \sigma_r^2 \sum_{j=1}^{N_r} \hat{\mathbf{h}}_k^H \mathbf{E}_j \widetilde{\mathbf{W}} \mathbf{E}_j^H \hat{\mathbf{h}}_k \geq \frac{\psi_k}{\xi_k(1-\rho_k)} - \sigma_k^2. \end{aligned} \quad (19)$$

TABLE I

AO-BASED NON-ROBUST TRANSCIVER DESIGN ALGORITHM

1. Initialize \mathbf{W} and define the tolerance of accuracy δ .
2. **Repeat**
 - 2.1 Solve problem (15) with fixed \mathbf{W} to obtain the updated $\{\mathbf{f}_k, \rho_k\}$.
 - 2.2 Solve problem (20) with fixed $\{\mathbf{f}_k, \rho_k\}$ to obtain the updated \mathbf{W} . Employ the proposed rank-one recovery method in Appendix A if higher-rank solutions are returned by solving problem (20).
3. **Until** the total power consumption between two adjacent iterations is less than δ or the total power consumption of step 2.2 is higher than that of step 2.1.

Hence, (13) can be reformulated as the following SDP problem by employing the well-known SDR technique

$$\begin{aligned} & \min_{\widetilde{\mathbf{W}}} \sum_{k=1}^K \left(\|\mathbf{f}_k\|^2 + \text{Tr}(\mathbf{C}_k \widetilde{\mathbf{W}} \mathbf{C}_k^H) \right) + \sigma_r^2 \text{Tr}(\widetilde{\mathbf{W}}) \\ & \text{s.t. (18) and (19), } \widetilde{\mathbf{W}} \succeq \mathbf{0}, \forall k \in \mathcal{K}, \end{aligned} \quad (20)$$

where $\mathbf{C}_k = (\mathbf{G} \mathbf{f}_k)^T \otimes \mathbf{I}_{N_r}$. Different from (15), the optimal solution $\widetilde{\mathbf{W}}^*$ to problem (20) is not necessarily rank-one; hence a simple rank-one recovery method based on a randomization procedure is proposed in Appendix A to address this issue.

The AO-based iterative algorithm to solve problem (13) is summarized in Table I. Note that in each iteration of this algorithm, the objective function can only be decreased⁴ and it is also lower bounded by zero, thus the convergence of the iterative algorithm is guaranteed.

B. Robust AO-Based Joint Transceiver Design

In this subsection, we address the robust counterpart of the non-robust AO-based joint transceiver design by employing the channel error model considered in Subsection II-B. We demonstrate that the corresponding subproblems can be converted to alternative forms where the concepts of SDR and S-procedure can be applied.

First, let us consider the optimization of $\{\mathbf{f}_k, \rho_k\}$ in (14) when \mathbf{W} is fixed under imperfect CSI, i.e. $\mathbf{h}_k = \hat{\mathbf{h}}_k + \mathbf{e}_k, \forall k \in \mathcal{K}$. In this case, the SINR constraints in (15) can be replaced by the following quadratic forms:

$$(\hat{\mathbf{h}}_k + \mathbf{e}_k)^H \mathbf{U}_k (\hat{\mathbf{h}}_k + \mathbf{e}_k) \geq \sigma_k^2 + \frac{\omega_k^2}{\rho_k}, \quad (21)$$

where \mathbf{e}_k satisfy (11) and \mathbf{U}_k can be expressed as

$$\mathbf{U}_k = \frac{1}{\gamma_k} \mathbf{Q}_k - \sum_{j \neq k} \mathbf{Q}_j - \sigma_r^2 \mathbf{W} \mathbf{W}^H. \quad (22)$$

Similarly, the EH constraints can be reformulated as the following expression:

$$(\hat{\mathbf{h}}_k + \mathbf{e}_k)^H \mathbf{V}_k (\hat{\mathbf{h}}_k + \mathbf{e}_k) + \sigma_k^2 \geq \frac{\psi_k}{\xi_k(1-\rho_k)}, \forall \|\mathbf{e}_k\|^2 \leq \eta_k^2, \quad (23)$$

⁴Due to the rank-one recovery method, the total transmission power of step 2.2 is not necessarily less than that of step 2.1. However, we can terminate the algorithm if that happens to ensure the convergence of the algorithm. Note that this rare situation does not happen in all our simulations.

where $\mathbf{V}_k = \sum_{j=1}^K \mathbf{Q}_j + \sigma_r^2 \mathbf{W} \mathbf{W}^H$.

By applying the S-procedure, the constraints in (21) and (23) can be reformulated as finite convex constraints, which are equivalent to the following two linear matrix inequality (LMI) constraints

$$\begin{bmatrix} \mathbf{U}_k + \lambda_k \mathbf{I} & \mathbf{U}_k \hat{\mathbf{h}}_k \\ \hat{\mathbf{h}}_k^H \mathbf{U}_k & \hat{\mathbf{h}}_k^H \mathbf{U}_k \hat{\mathbf{h}}_k - \sigma_k^2 - \omega_k^2 p_k - \lambda_k \eta_k^2 \end{bmatrix} \succeq \mathbf{0}, \quad (24)$$

$$\begin{bmatrix} \mathbf{V}_k + \mu_k \mathbf{I} & \mathbf{V}_k \hat{\mathbf{h}}_k \\ \hat{\mathbf{h}}_k^H \mathbf{V}_k & \hat{\mathbf{h}}_k^H \mathbf{V}_k \hat{\mathbf{h}}_k + \sigma_k^2 - \frac{\psi_k}{\xi_k} q_k - \mu_k \eta_k^2 \end{bmatrix} \succeq \mathbf{0}, \quad (25)$$

where $p_k = \frac{1}{\rho_k}$, $q_k = \frac{1}{1-\rho_k}$, while $\lambda_k \geq 0$ and $\mu_k \geq 0$ are slack variables.

With (24) and (25), the robust counterpart of problem (15) can be reformulated as follows by ignoring the rank-one constraints for all \mathbf{F}_k 's:

$$\begin{aligned} \min_{\{\mathbf{F}_k, p_k, q_k, \lambda_k, \mu_k\}} & \sum_{k=1}^K \text{Tr}(\mathbf{F}_k) + \sum_{k=1}^K \text{Tr}(\mathbf{Q}_k) + \sigma_r^2 \|\mathbf{W}\|^2 \\ \text{s.t.} & \text{ (24) and (25), } \lambda_k \geq 0, \mu_k \geq 0, \\ & p_k \geq 1, q_k \geq 1, \text{invp}(p_k) + \text{invp}(q_k) \leq 1, \\ & \mathbf{F}_k \succeq \mathbf{0}, \forall k \in \mathcal{K}. \end{aligned} \quad (26)$$

It is worth noting that different from problem (15) which always returns a rank-one solution, the optimal solution $\{\mathbf{F}_k^*\}$ of (26) may not be of rank-one, in which case, additional processing steps may be needed to extract a rank-one solution from the \mathbf{F}_k^* . To this end, a rank-one recovery method based on a randomization procedure but with lower complexity is presented in Appendix A.

Next, we consider the optimization of the RS AF matrix \mathbf{W} with fixed $\{\mathbf{f}_k, \rho_k\}$. Similar to Subsection III-A, we have the following expression

$$\begin{aligned} \mathbf{g}_{kj} &= \text{vec}(\text{conj}(\mathbf{h}_k) \mathbf{f}_j^T \mathbf{G}^T) = (\mathbf{G} \mathbf{f}_j \otimes \mathbf{I}_{N_r}) \text{conj}(\mathbf{h}_k) \\ &= \hat{\mathbf{G}}_j \text{conj}(\mathbf{h}_k), \end{aligned} \quad (27)$$

where $\hat{\mathbf{G}}_j = \mathbf{G} \mathbf{f}_j \otimes \mathbf{I}_{N_r}$, $j \in \mathcal{K}$. Thus, the robust version of (18) can be formulated as

$$\begin{aligned} & \frac{1}{\gamma_k} (\hat{\mathbf{h}}_k^H + \mathbf{e}_k^H) \overline{\mathbf{W}}_k (\hat{\mathbf{h}}_k + \mathbf{e}_k) \\ & - \sum_{j \neq k}^K (\hat{\mathbf{h}}_k^H + \mathbf{e}_k^H) \overline{\mathbf{W}}_j (\hat{\mathbf{h}}_k + \mathbf{e}_k) \\ & - \sigma_r^2 \sum_{j=1}^{N_r} (\hat{\mathbf{h}}_k^H + \mathbf{e}_k^H) \mathbf{E}_j \widetilde{\mathbf{W}} \mathbf{E}_j^H (\hat{\mathbf{h}}_k + \mathbf{e}_k) \\ & \geq \sigma_k^2 + \frac{\omega_k^2}{\rho_k}, \forall \|\mathbf{e}_k\|^2 \leq \eta_k^2, k \in \mathcal{K}, \end{aligned} \quad (28)$$

where $\overline{\mathbf{W}}_j = \hat{\mathbf{G}}_j^T \widetilde{\mathbf{W}} \text{conj}(\hat{\mathbf{G}}_j)$, and $\widetilde{\mathbf{W}}$ has already been defined in Subsection III-A. By applying the S-procedure, we can transform (28) into the following LMIs

$$\begin{bmatrix} \tilde{\mathbf{U}}_k + \lambda_k \mathbf{I} & \tilde{\mathbf{U}}_k \hat{\mathbf{h}}_k \\ \hat{\mathbf{h}}_k^H \tilde{\mathbf{U}}_k & \hat{\mathbf{h}}_k^H \tilde{\mathbf{U}}_k \hat{\mathbf{h}}_k - \sigma_k^2 - \omega_k^2 p_k - \lambda_k \eta_k^2 \end{bmatrix} \succeq \mathbf{0}, \quad (29)$$

TABLE II
AO-BASED ROBUST TRANSCEIVER DESIGN ALGORITHM

-
1. Initialize \mathbf{W} and define the tolerance of accuracy δ .
 2. **Repeat**
 - 2.1 Solve problem (26) with fixed \mathbf{W} to obtain the updated $\{\mathbf{F}_k, \rho_k\}$. If $\{\mathbf{F}_k\}$ are rank-one matrices, use their principal eigenvectors as a solution. Otherwise, employ the rank-one recovery method to recover a rank-one solution from $\{\mathbf{F}_k\}$.
 - 2.2 Solve problem (31) with fixed $\{\mathbf{F}_k, \rho_k\}$ to obtain the updated \mathbf{W} . If $\widetilde{\mathbf{W}}$ is a rank-one matrix, use its principal eigenvector as a solution. Otherwise, employ the method in Appendix A to recover a rank-one solution from $\widetilde{\mathbf{W}}$.
 3. **Until** the total power consumption between two adjacent iterations is less than δ or increased.
-

where $\tilde{\mathbf{U}}_k = \frac{1}{\gamma_k} \overline{\mathbf{W}}_k - \sum_{j \neq k}^K \overline{\mathbf{W}}_j - \sigma_r^2 \sum_{k=1}^{N_r} \mathbf{E}_k \widetilde{\mathbf{W}} \mathbf{E}_k^H$ and $\lambda_k \geq 0$.

Similarly, the robust version of (19) can be formulated as

$$\begin{bmatrix} \tilde{\mathbf{V}}_k + \mu_k \mathbf{I} & \tilde{\mathbf{V}}_k \hat{\mathbf{h}}_k \\ \hat{\mathbf{h}}_k^H \tilde{\mathbf{V}}_k & \hat{\mathbf{h}}_k^H \tilde{\mathbf{V}}_k \hat{\mathbf{h}}_k + \sigma_k^2 - \frac{\psi_k}{\xi_k} q_k - \mu_k \eta_k^2 \end{bmatrix} \succeq \mathbf{0}, \quad (30)$$

where $\tilde{\mathbf{V}}_k = \sum_{j=1}^K \overline{\mathbf{W}}_j + \sigma_r^2 \sum_{k=1}^{N_r} \mathbf{E}_k \widetilde{\mathbf{W}} \mathbf{E}_k^H$ and $\mu_k \geq 0$. Hence,

problem (14) with fixed $\{\mathbf{f}_k, \rho_k\}$ can be formulated as the following SDP problem with the SDR technique

$$\begin{aligned} \min_{\widetilde{\mathbf{W}}, \{\lambda_k, \mu_k\}} & \sum_{k=1}^K \left(\|\mathbf{f}_k\|^2 + \text{Tr}(\mathbf{C}_k \widetilde{\mathbf{W}} \mathbf{C}_k^H) \right) + \sigma_r^2 \text{Tr}(\widetilde{\mathbf{W}}) \\ \text{s.t.} & \text{ (29) and (30), } \widetilde{\mathbf{W}} \succeq \mathbf{0}, \lambda_k \geq 0, \mu_k \geq 0, \forall k, \end{aligned} \quad (31)$$

where \mathbf{C}_k has been defined in Subsection III-A. Note that the optimal solution of (31) is also not necessarily rank-one and thus we can employ the method in Appendix A to address this issue.

We summarize the AO-based robust joint transceiver design algorithm in Table II. For practical implementation, the optimally designed AF matrix \mathbf{W} and PS ratios $\{\rho_k\}$ should be fed forward from the BS to the RS and receivers, respectively, through signaling channels prior to data transmission.

IV. SWITCHED RELAYING BASED JOINT TRANSCEIVER DESIGN

In the previous section, we proposed novel AO-based transceiver design algorithms. As will be shown in Section VI, these algorithms can achieve an excellent performance in transmission, but they are characterized by higher signaling overhead and computational complexity. In this section, motivated by these considerations, we develop alternative SR-based transceiver design algorithms that are more efficient and simpler to implement. As illustrated in Fig. 2, we equip the RS with a finite codebook of permutation matrices⁵, i.e., $\Upsilon = \{\mathbf{T}_1, \mathbf{T}_2, \dots, \mathbf{T}_B\}$, where $\mathbf{T}_l \in \{0, 1\}^{N_r \times N_r}$ is the l -th matrix in the codebook, index $l \in \{1, \dots, B\}$ and B denotes

⁵A permutation matrix is a square binary matrix that has exactly one entry equal to 1 in each row and each column, while all the other entries are equal to 0.

the codebook size which satisfies $B \ll N_r!$.⁶ In order to reduce the signaling overhead and the number of optimization variables, the RS AF matrix \mathbf{W} is constructed by multiplying the appropriate permutation matrix from the codebook with a power scaling factor. That is to say, the optimization of \mathbf{W} is replaced by $\sqrt{\beta_l}\mathbf{T}_l$, where β_l is a variable power scaling factor. Thus, each permutation matrix gives rise to a permuted channel matrix for which we can design a so-called *latent* transceiver, consisting of the BS beamforming vectors, the RS power scaling factor and the receiver PS ratios. Among the B latent transceivers so designed, by an algorithm to be developed below, the optimal one with index l_{opt} is chosen by means of a suitable selection criterion for transmission. Specifically, the selection mechanism is designed to choose the optimal latent transceiver with the minimum power consumption, which can be expressed as

$$l_{opt} = \arg \min_l P_l, \quad (32)$$

where P_l denotes the total transmission power corresponding to the l th latent transceiver.

Before data transmission, the BS only sends the index of the permutation matrix, the RS power scaling factor and the receiver PS ratios corresponding to the optimum transceiver to the RS and the receivers. Compared to the AO-based algorithms, the SR-based algorithms can significantly reduce the number of signaling bits and the computational complexity. The proposed SR-based scheme works as follows.

- The BS designs the B latent transceivers based on available permutation matrices within the codebook; it then determines the optimal latent transceiver based on (32).
- The BS sends the optimal permutation index l_{opt} , the corresponding RS power scaling factor, and the PS ratios corresponding to the optimal transceiver to the RS and the receivers through signaling channels.
- The RS constructs the optimal RS AF matrix based on the forwarded RS power scaling factor and the stored permutation matrix with index l_{opt} .

We introduce the non-robust and robust latent transceiver design algorithms in Subsection IV-A and IV-B, respectively. In Subsection IV-C, a simplified SR-based transceiver design algorithm is proposed. The design approach for the codebook of permutation matrices is presented in Subsection IV-D.

A. Non-Robust Latent Transceiver Design

Firstly, we introduce a non-robust algorithm to construct the l th latent transceiver. We aim to design the beamforming vectors $\{\mathbf{f}_k^l\}$, the RS power scaling factor β_l and the receiver PS ratios $\{\rho_k^l\}$ so as to minimize the sum of BS and RS transmit power under both SINR and EH constraints. We note that superscripts l in $\{\mathbf{f}_k^l\}$, $\{\rho_k^l\}$, etc., have been removed in the

⁶The total number of permutation matrices at the RS is $N_r!$. It is not realistic to use all the permutation matrices as the codebook when N_r is large. Thus, we propose to construct a codebook of permutation matrices with B elements, $B \ll N_r!$. The codebook design approach will be introduced in Subsection IV-D. In practice, the value of B should be chosen to achieve a suitable tradeoff between performance requirements and implementation complexity.

following for notational simplicity. For each latent transceiver, the optimization problem can be formulated as

$$\begin{aligned} & \min_{\{\mathbf{f}_k, \rho_k\}, \beta_l} P_B + P_R \\ & \text{s.t. } \Gamma_k \geq \gamma_k, P_k^{\text{EH}} \geq \psi_k, \\ & 0 \leq \rho_k \leq 1, \mathbf{W} = \sqrt{\beta_l}\mathbf{T}_l, \forall k \in \mathcal{K}. \end{aligned} \quad (33)$$

As we can see, although we replaced the AF matrix \mathbf{W} with $\sqrt{\beta_l}\mathbf{T}_l$, problem (33) is still non-convex and difficult to solve due to the coupling between variables \mathbf{f}_k , ρ_k and β_l . Our proposed method is motivated by the observation that problem (33) can be reformulated as a difference of convex (DC) programming problem with proper transformations. Thus, the concept of CCCP [25], [26] can be adopted to iteratively solve the DC problem, as explained below.

First, we introduce the variable substitution

$$\varphi_l = \frac{1}{\beta_l}, \quad (34)$$

and further define the following vectors:

$$\begin{aligned} \mathbf{p} &= [p_1, \dots, p_K]^T, \quad \mathbf{q} = [q_1, \dots, q_K]^T, \\ \mathbf{f} &= [\mathbf{f}_1^T, \dots, \mathbf{f}_K^T]^T, \quad \mathbf{r} = [\mathbf{p}^T, \mathbf{q}^T, \varphi_l, \mathbf{f}^T]^T, \end{aligned} \quad (35)$$

where p_k and q_k have already been introduced in Subsection III-B, alongside with (24) and (25). Then, the objective function of problem (33) can be transformed into

$$P_l(\mathbf{r}) = \sum_{k=1}^K \mathbf{f}_k^H \mathbf{f}_k + \sum_{k=1}^K \frac{\mathbf{f}_k^H \mathbf{G}^H \mathbf{G} \mathbf{f}_k}{\varphi_l} + \sigma_r^2 \frac{1}{\varphi_l}, \quad (36)$$

which is strictly jointly convex in the variables $\{\varphi_l, \mathbf{f}\} \in \mathbb{R}_+ \times \mathbb{C}^{KN_t \times 1}$ [22].

Similar to the transformation of the objective function, the SINR constraints can be rewritten as

$$w_k(\mathbf{r}) - x_k(\mathbf{r}) \leq 0, \quad (37)$$

where $w_k(\mathbf{r})$ and $x_k(\mathbf{r})$ are defined as

$$w_k(\mathbf{r}) = \sum_{j \neq k} \mathbf{f}_j^H \mathbf{G}^H \mathbf{T}_l^H \hat{\mathbf{h}}_k \hat{\mathbf{h}}_k^H \mathbf{T}_l \mathbf{G} \mathbf{f}_j \quad (38)$$

$$+ \sigma_k^2 \varphi_l + \sigma_r^2 \hat{\mathbf{h}}_k^H \hat{\mathbf{h}}_k + \frac{1}{4} \omega_k^2 (p_k + \varphi_l)^2,$$

$$x_k(\mathbf{r}) = \frac{1}{4} \omega_k^2 (p_k - \varphi_l)^2 + \frac{1}{\gamma_k} \mathbf{f}_k^H \mathbf{G}^H \mathbf{T}_l^H \hat{\mathbf{h}}_k \hat{\mathbf{h}}_k^H \mathbf{T}_l \mathbf{G} \mathbf{f}_k. \quad (39)$$

Moreover, the EH constraints can be recast as

$$y_k(\mathbf{r}) - z_k(\mathbf{r}) \leq 0, \quad (40)$$

where

$$y_k(\mathbf{r}) = \frac{\psi_k}{4\xi_k} (q_k + \varphi_l)^2 - \sigma_r^2 \hat{\mathbf{h}}_k^H \hat{\mathbf{h}}_k, \quad (41)$$

$$z_k(\mathbf{r}) = \sum_{j=1}^K \mathbf{f}_j^H \mathbf{G}^H \mathbf{T}_l^H \hat{\mathbf{h}}_k \hat{\mathbf{h}}_k^H \mathbf{T}_l \mathbf{G} \mathbf{f}_j \quad (42)$$

$$+ \sigma_k^2 \varphi_l + \frac{\psi_k}{4\xi_k} (q_k - \varphi_l)^2.$$

We remark that (38), (39), (41) and (42) are all convex functions jointly with respect to the variables in $\mathbf{r} \in \mathbb{R}_+^K \times$

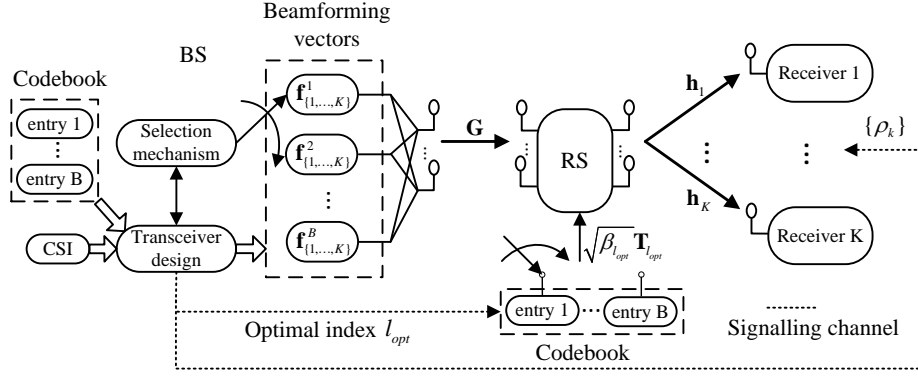


Fig. 2. Proposed transceiver scheme with switched relaying processing for multiuser MISO relay system. The dashed line denotes signaling channels.

$\mathbb{R}_+^K \times \mathbb{R}_+ \times \mathbb{C}^{KN_t \times 1}$. Thus, problem (33) can be equivalently reformulated as the following DC program:

$$\begin{aligned} \min_{\mathbf{r}} \quad & P_l(\mathbf{r}) \\ \text{s.t.} \quad & w_k(\mathbf{r}) - x_k(\mathbf{r}) \leq 0, \quad y_k(\mathbf{r}) - z_k(\mathbf{r}) \leq 0, \\ & p_k \geq 1, \quad q_k \geq 1, \quad \text{invp}(p_k) + \text{invp}(q_k) \leq 1, \quad \forall k \in \mathcal{K}, \end{aligned} \quad (43)$$

where the last set of inequality constraints must be satisfied with equality at optimality, for otherwise, the objective value can be further decreased by decreasing the p_k 's.

According to the concept of CCCP, we approximate the functions $x_k(\mathbf{r})$ and $z_k(\mathbf{r})$ in the i th iteration by their first-order Taylor expansions around the current point $\mathbf{r}^{(i)}$, denoted as $\hat{x}_k(\mathbf{r}^{(i)}, \mathbf{r})$ and $\hat{z}_k(\mathbf{r}^{(i)}, \mathbf{r})$, respectively. With the help of [38] and [39], $\hat{x}_k(\mathbf{r}^{(i)}, \mathbf{r})$ is given by

$$\hat{x}_k(\mathbf{r}^{(i)}, \mathbf{r}) = x_k(\mathbf{r}^{(i)}) + 2\mathcal{R}\{\nabla x_k(\mathbf{r}^{(i)})^H(\mathbf{r} - \mathbf{r}^{(i)})\}, \quad (44)$$

where $\nabla x_k(\mathbf{r}^{(i)})$ denotes the conjugate derivative of the function $x_k(\mathbf{r})$ with respect to the complex vector \mathbf{r} .⁷ We note that $\hat{x}_k(\mathbf{r}^{(i)}, \mathbf{r})$ is an affine function of \mathbf{r} . $\nabla x_k(\mathbf{r}^{(i)})$ is given by

$$\begin{aligned} \nabla x_k(\mathbf{r}^{(i)}) = & [\mathbf{0}_{1 \times (k-1)}, \frac{1}{4}\omega_k^2(p_k^{(i)} - \varphi_l^{(i)}), \mathbf{0}_{1 \times (2K-k)}, \\ & -\frac{1}{4}\omega_k^2(p_k^{(i)} - \varphi_l^{(i)}), \frac{1}{\gamma_k}(\mathbf{G}^H \mathbf{T}_l^H \hat{\mathbf{h}}_k \hat{\mathbf{h}}_k^H \mathbf{T}_l \mathbf{G} \mathbf{f}_k^{(i)})^T]^T. \end{aligned} \quad (45)$$

Similarly, $\hat{z}_k(\mathbf{r}^{(i)}, \mathbf{r})$ can be expressed as

$$\hat{z}_k(\mathbf{r}^{(i)}, \mathbf{r}) = z_k(\mathbf{r}^{(i)}) + 2\mathcal{R}\{\nabla z_k(\mathbf{r}^{(i)})^H(\mathbf{r} - \mathbf{r}^{(i)})\}, \quad (46)$$

where

$$\begin{aligned} \nabla z_k(\mathbf{r}^{(i)}) = & [\mathbf{0}_{1 \times (K+k-1)}, \frac{\psi_k}{4\xi_k}(q_k^{(i)} - \varphi_l^{(i)}), \mathbf{0}_{1 \times (K-k)}, \\ & \frac{1}{2}\sigma_k^2 - \frac{\psi_k}{4\xi_k}(q_k^{(i)} - \varphi_l^{(i)}), (\tilde{\mathbf{G}}_k \mathbf{f}_1^{(i)})^T, \dots, (\tilde{\mathbf{G}}_k \mathbf{f}_K^{(i)})^T]^T, \\ \tilde{\mathbf{G}}_k = & \mathbf{G}^H \mathbf{T}_l^H \hat{\mathbf{h}}_k \hat{\mathbf{h}}_k^H \mathbf{T}_l \mathbf{G}. \end{aligned} \quad (47)$$

Then, in the i th iteration of the proposed CCCP based algorithm, we have the following convex optimization problem

$$\begin{aligned} \min_{\mathbf{r}} \quad & P_l(\mathbf{r}) \\ \text{s.t.} \quad & w_k(\mathbf{r}) - \hat{x}_k(\mathbf{r}^{(i)}, \mathbf{r}) \leq 0, \quad y_k(\mathbf{r}) - \hat{z}_k(\mathbf{r}^{(i)}, \mathbf{r}) \leq 0, \\ & p_k \geq 1, \quad q_k \geq 1, \quad \text{invp}(p_k) + \text{invp}(q_k) \leq 1, \quad \forall k \in \mathcal{K}, \end{aligned} \quad (48)$$

whose solution is denoted by $\mathbf{r}^{(i+1)}$.

⁷Since \mathbf{r} is composed of both real and complex variables, we make a modification of $\nabla x_k(\mathbf{r}^{(i)})$ such that (44) holds for \mathbf{r} .

TABLE III
NON-ROBUST LATENT TRANSCIVER DESIGN ALGORITHM

1. Define the tolerance of accuracy δ and the maximum number of iteration N_{max} .
2. **For** $l = 1, \dots, B$
3. - Initialize the algorithm with a feasible point $\mathbf{r}^{(0)}$ which is obtained by solving problem (33) with $\mathbf{W} = \mathbf{T}_l$. Set the iteration number $i = 0$.
4. - **Repeat**
- Compute the affine approximation $\hat{x}_k(\mathbf{r}^{(i)}, \mathbf{r})$ and $\hat{z}_k(\mathbf{r}^{(i)}, \mathbf{r})$ according to (44) and (46), respectively.
- Solve problem (49), and assign the solution to $\mathbf{r}^{(i+1)}$.
- Update the iteration number : $i = i + 1$.
- **Until** $|P_l(\mathbf{r}^{(i+1)}) - P_l(\mathbf{r}^{(i)})| \leq \delta$ or the maximum number of iterations is reached, i.e., $i > N_{max}$.
5. - Obtain the l th latent transceiver $\{\mathbf{f}_k^*, \rho_k^*, \beta_l^*\}$.
6. **End**

Proposition 1: By introducing a new set of variables d_k , \tilde{d}_k , e_k and \tilde{e}_k , $k \in \mathcal{K}$, problem (48) can be reformulated as the following SOCP problem

$$\begin{aligned} \min_{\mathbf{r}, P_1, P_2, P_3} \quad & P_1 + P_2 + P_3 \\ \text{s.t.} \quad & \|[\mathbf{f}_1^T, \dots, \mathbf{f}_K^T, (P_1 - 1)/2]\| \leq (P_1 + 1)/2, \\ & \|[(\mathbf{G}\mathbf{f}_1)^T, \dots, (\mathbf{G}\mathbf{f}_K)^T, (P_2 - \varphi_l)/2]\| \leq (P_2 + \varphi_l)/2, \\ & \| [2\sigma_r, \varphi_l - P_3] \| \leq \varphi_l + P_3, \\ & \| [\mathbf{w}_k^T, \frac{\tilde{d}_k - d_k - 1}{2}] \| \leq \frac{\tilde{d}_k - d_k + 1}{2}, \quad \forall k, \\ & \| [\sqrt{\frac{\psi_k}{4\xi_k}}(q_k + \varphi_l), \frac{\tilde{e}_k - e_k - 1}{2}] \| \leq \frac{\tilde{e}_k - e_k + 1}{2}, \\ & p_k \geq 1, \quad q_k \geq 1, \quad \text{invp}(p_k) + \text{invp}(q_k) \leq 1, \quad \forall k \in \mathcal{K}, \end{aligned} \quad (49)$$

where \mathbf{w}_k is defined in (71).

Proof: Please refer to Appendix B.

We can show that the proposed CCCP based iterative algorithm for the l th transceiver design converges to a local optimal solution of problem (33). The proof is similar to that of Lemma 2 and Theorem 1 in [39], and we therefore omit the details. We summarize the proposed non-robust latent transceiver design algorithm in Table III.

B. Robust Latent Transceiver Design

Secondly, let us propose a robust latent transceiver design algorithm by taking the channel errors into consideration. As

we can see, the concept of SR can also be applied to problem (14), which can be reformulated as follows:

$$\begin{aligned} & \min_{\{\mathbf{f}_k, \rho_k\}, \beta_l} P_B + P_R \\ & \text{s.t. } \Gamma_k \geq \gamma_k, P_k^{\text{EH}} \geq \psi_k, 0 \leq \rho_k \leq 1, \\ & \mathbf{W} = \sqrt{\beta_l} \mathbf{T}_l, \|\mathbf{e}_k\|^2 \leq \eta_k^2, \forall k \in \mathcal{K}. \end{aligned} \quad (50)$$

We employ a subgradient-type iterative algorithm to solve this problem. Our proposed method is motivated by the observation that, if we fix β_l , then problem (50) is equivalent to problem (26) with the SDR technique.⁸ With fixed β_l , (24) and (25) can be reformulated as the following two LMIs:

$$\begin{bmatrix} \bar{\mathbf{U}}_k + \lambda_k \mathbf{I} & \bar{\mathbf{U}}_k \hat{\mathbf{h}}_k \\ \hat{\mathbf{h}}_k^H \bar{\mathbf{U}}_k & \hat{\mathbf{h}}_k^H \bar{\mathbf{U}}_k \hat{\mathbf{h}}_k - \frac{\sigma_k^2}{\beta_l} - \frac{\omega_k^2 p_k}{\beta_l} - \lambda_k \eta_k^2 \end{bmatrix} \succeq \mathbf{0}, \quad (51)$$

$$\begin{bmatrix} \bar{\mathbf{V}}_k + \mu_k \mathbf{I} & \bar{\mathbf{V}}_k \hat{\mathbf{h}}_k \\ \hat{\mathbf{h}}_k^H \bar{\mathbf{V}}_k & \hat{\mathbf{h}}_k^H \bar{\mathbf{V}}_k \hat{\mathbf{h}}_k + \frac{\sigma_k^2}{\beta_l} - \frac{\psi_k}{\xi_k \beta_l} q_k - \mu_k \eta_k^2 \end{bmatrix} \succeq \mathbf{0}, \quad (52)$$

where $\bar{\mathbf{U}}_k = \frac{1}{\gamma_k} \tilde{\mathbf{Q}}_k - \sum_{j \neq k} \tilde{\mathbf{Q}}_j - \sigma_r^2 \mathbf{I}$, $\bar{\mathbf{V}}_k = \sum_{j=1}^K \tilde{\mathbf{Q}}_j + \sigma_r^2 \mathbf{I}$, and $\tilde{\mathbf{Q}}_k = \mathbf{T}_l \mathbf{G} \mathbf{F}_k \mathbf{G}^H \mathbf{T}_l^H$.

Then, problem (50) with the use of the SDR technique and fixed β_l can be expressed as

$$\begin{aligned} & f(\beta_l) = \\ & \min_{\{\mathbf{F}_k, p_k, q_k, \lambda_k, \mu_k\}} \sum_{k=1}^K \text{Tr}(\mathbf{F}_k) + \beta_l \sum_{k=1}^K \text{Tr}(\tilde{\mathbf{Q}}_k) + \sigma_r^2 \beta_l \\ & \text{s.t. (51) and (52), } \lambda_k \geq 0, \mu_k \geq 0, \\ & p_k \geq 1, q_k \geq 1, \text{invp}(p_k) + \text{invp}(q_k) \leq 1, \\ & \mathbf{F}_k \succeq \mathbf{0}, \forall k \in \mathcal{K}. \end{aligned} \quad (53)$$

We here consider the SDR version of problem (50) instead of its original form with rank-one constraints, since strong duality holds if problem (53) is feasible. The partial dual problem of (53) can be formulated as (54) shown at the top of next page, where $\mathbf{X}_k = \begin{bmatrix} \bar{\mathbf{X}}_k & \mathbf{x}_k \\ \mathbf{x}_k^H & x_k \end{bmatrix}$ and $\mathbf{Y}_k = \begin{bmatrix} \bar{\mathbf{Y}}_k & \mathbf{y}_k \\ \mathbf{y}_k^H & y_k \end{bmatrix}$ denote the dual variables associated with constraints (51) and (52), respectively. It is worth noting that \mathbf{X}_k and \mathbf{Y}_k can be obtained as side information provided with any standard SDP solver, since dual variables are served as a certificate for optimality.

Next, we can use the subgradient method [40] to iteratively solve the SDR version of problem (50). At the $(i+1)$ th iteration, the power scaling factor β_l can be updated according to

$$\beta_l(i+1) = [\beta_l(i) - \theta(i)s(i)]_{\varepsilon}^+, \quad (55)$$

where $[\cdot]_{\varepsilon}^+ = \max(\cdot, \varepsilon)$, $\theta(i)$ is the step-size in the i th iteration and $s(i)$ denotes a subgradient of $f(\beta_l)$ at $\beta_l(i)$. The

⁸The concept of CCCP can also be applied to the robust problem (50). However, based on simulations we find that the performance of the CCCP based algorithm is inferior to that of the subgradient-type algorithm. Thus, we employ the subgradient-type algorithm instead.

TABLE IV
ROBUST LATENT TRANSCIEVER DESIGN ALGORITHM

-
1. Initialize the step-size θ , define the tolerance of accuracy δ and the maximum number of iterations N_{max} .
 2. **For** $l = 1, \dots, B$
 3. Initialize $\beta_l(0)$. Set the iteration number $i = 0$.
 4. - **Repeat**
 5. - Solve problem (53) to obtain the optimal $\{\mathbf{F}_k^*, \rho_k^*\}$ and the corresponding dual variables $\{x_k^*, y_k^*\}$.
 6. - Update the power scaling factor according to (55).
 7. - Update the iteration number : $i = i + 1$.
 8. - **Until** $|f(\beta_l(i+1)) - f(\beta_l(i))| \leq \delta$ or the maximum number of iterations is reached, i.e., $i > N_{max}$.
 9. - Obtain the l th latent transceiver $\{\mathbf{f}_k^*, \rho_k^*, \beta_l^*\}$.
 6. **End**
-

subgradient $s(i)$ can be calculated as [41]

$$\begin{aligned} s(i) = & \sum_{k=1}^K \text{Tr}(\tilde{\mathbf{Q}}_k^*) + \sigma_r^2 - \sum_{k=1}^K x_k^* \left(\frac{\sigma_k^2}{\beta_l(i)^2} + \frac{\omega_k^2}{\rho_k^* \beta_l(i)^2} \right) \\ & + \sum_{k=1}^K y_k^* \left(\frac{\sigma_k^2}{\beta_l(i)^2} - \frac{\psi_k}{(1 - \rho_k^*) \xi_k \beta_l(i)^2} \right), \end{aligned} \quad (56)$$

where $\tilde{\mathbf{Q}}_k^* = \mathbf{T}_l \mathbf{G} \mathbf{F}_k^* \mathbf{G}^H \mathbf{T}_l^H$, $\{\mathbf{F}_k^*, \rho_k^*\}$ denotes the optimal solution of problem (53) and $\{x_k^*, y_k^*\}$ denote the lower right corner elements of \mathbf{X}_k^* and \mathbf{Y}_k^* , which are the optimal dual variables associated with (51) and (52).

Finally, the robust latent transceiver design algorithm is summarized in Table IV.⁹

C. Proposed Simplified SR-based Transceiver Design

As shown in Subsection IV-A and IV-B, the proposed SR-based transceiver design algorithm involves devising B latent transceivers corresponding to the elements in Υ where for each transceiver, we employ iterative methods to address the highly non-convex problem. Specifically, the design of each transceiver involves an iterative algorithm to obtain the corresponding BS beamforming vectors, RS power scaling factor and receiver PS ratios. However, for given CSIs only the best transceiver with the minimum total power consumption is selected for transmission according to the selection mechanism (32) while the other $B-1$ solutions are discarded. Thus, there will be a considerable waste in the computational resources. In order to improve the proposed SR-based transceiver design algorithm and make it more suitable for practical implementation, we propose a heuristic approach, referred to as the *simplified* latent transceiver design algorithm, to address the aforementioned problem. Based on simulation experiments, we find that a good initial point obtained by solving problem (33) or (50) with fixed initial power scaling factor β_l almost always leads to a better convergent point than by solving

⁹For the non-robust case, we can also employ the subgradient method to address problem (33) with each subproblem being an SDP problem. It is well known that solving an SDP problem requires relatively high computational complexity compared with solving an SOCP problem. Moreover, it is important to note that the two algorithms for the non-robust case have very close performance in our simulations. Thus, we employ the CCCP based algorithm for the non-robust case.

$$\begin{aligned}
f(\beta_l) = & \max_{\{\mathbf{X}_k, \mathbf{Y}_k\}} \min_{\{\mathbf{F}_k, \rho_k\}} - \sum_{k=1}^K \text{Tr} \left(\mathbf{X}_k \begin{bmatrix} \bar{\mathbf{U}}_k + \lambda_k \mathbf{I} & \bar{\mathbf{U}}_k \hat{\mathbf{h}}_k \\ \hat{\mathbf{h}}_k^H \bar{\mathbf{U}}_k & \hat{\mathbf{h}}_k^H \bar{\mathbf{U}}_k \hat{\mathbf{h}}_k - \frac{\sigma_k^2}{\beta_l} - \frac{\omega_k^2 \alpha_k}{\beta_l} - \lambda_k \eta_k^2 \end{bmatrix} \right) \\
& - \sum_{k=1}^K \text{Tr} \left(\mathbf{Y}_k \begin{bmatrix} \bar{\mathbf{V}}_k + \mu_k \mathbf{I} & \bar{\mathbf{V}}_k \hat{\mathbf{h}}_k \\ \hat{\mathbf{h}}_k^H \bar{\mathbf{V}}_k & \hat{\mathbf{h}}_k^H \bar{\mathbf{V}}_k \hat{\mathbf{h}}_k + \frac{\sigma_k^2}{\beta_l} - \frac{\psi_k}{\xi_k \beta_l} \beta_k - \mu_k \eta_k^2 \end{bmatrix} \right) + \sum_{k=1}^K \text{Tr}(\mathbf{F}_k) + \beta_l \sum_{k=1}^K \text{Tr}(\tilde{\mathbf{Q}}_k) + \sigma_r^2 \beta_l,
\end{aligned} \tag{54}$$

TABLE V
SIMPLIFIED NON-ROBUST LATENT TRANSCIEVER DESIGN ALGORITHM

1. Define the tolerance of accuracy δ and the maximum iteration number N_{max} .
2. **For** the l th latent transceiver ($l = 1, \dots, B$)
3. - Compute a initial feasible point $\mathbf{r}^{(0)}$ which is obtained by solving problem (33) with $\mathbf{W} = \mathbf{T}_l$.
4. **end**
5. Choose the initial $\mathbf{r}^{(0)}$ and $\mathbf{T}_{l_{opt}}$ with the minimum objective value. Set the iteration number $i = 0$.
6. **Repeat**
 - Compute the affine approximation $\hat{x}_k(\mathbf{r}^{(i)}, \mathbf{r})$ and $\hat{z}_k(\mathbf{r}^{(i)}, \mathbf{r})$ according to (44) and (46), respectively.
 - Solve problem (49), and assign the solution to $\mathbf{r}^{(i+1)}$.
 - Update the iteration number : $i = i + 1$.
7. **Until** $|P_{l_{opt}}(\mathbf{r}^{(i+1)}) - P_{l_{opt}}(\mathbf{r}^{(i)})| \leq \delta$ or the maximum number of iterations is reached, i.e., $i > N_{max}$.

with a not so good initial point. Thus, we only design the particular transceiver with the best initial point. The proposed simplified non-robust latent transceiver design algorithm is summarized in Table V. The robust version of the simplified latent transceiver design algorithm is similar to the non-robust case, and thus is omitted here. We will show in Section VI that the simplified SR-based transceiver design algorithms can achieve a similar performance with that of the proposed SR-based algorithms in Table III and IV.

D. Codebook Design

In this subsection, we propose two algorithms to construct the codebook of permutation matrices. The basic principle of the proposed algorithms is to choose the permutation matrices which are more likely to result in lower transmission power. We make a promising observation that when the singular values of the permuted channel matrix $\mathbf{H}\mathbf{T}_l\mathbf{G}$ are larger or more equally distributed, the total power consumption is usually smaller, where the channel matrix \mathbf{H} has already been defined in Subsection II-C and $\mathbf{H}\mathbf{T}_l\mathbf{G}$ represents the equivalent channel matrix between the BS and the receivers.

Let π_k^l denotes the k th singular value of $\mathbf{H}\mathbf{T}_l\mathbf{G}$, $k \in \mathcal{K}$. The first scheme (referred to as *Sum-Max* method) constructs the codebook of permutation matrices by choosing the ones which correspond to the B largest sums of singular values, i.e.,

$$\{\mathbf{T}_1, \dots, \mathbf{T}_B\} = \arg \max_{\mathbf{T}_l} \mathbf{B} \left(\sum_{k=1}^K \pi_k^l \right), \tag{57}$$

where $\max_{\mathbf{B}}(\cdot)$ returns the permutation matrices correspond to the B largest values of its argument.

Alternatively, the second scheme (referred to as *Max-Min* method) chooses the permutation matrices to maximize the

smallest singular value, i.e.,

$$\{\mathbf{T}_1, \dots, \mathbf{T}_B\} = \arg \max_{\mathbf{T}_l} \mathbf{B} \left(\min_{k \in \mathcal{K}} (\pi_k^l) \right). \tag{58}$$

It is worth noting that the proposed two schemes are heuristic techniques which may serve as a shortcut to the process of finding a satisfactory solution. The performance of the codebook design algorithms will be studied in the simulation results in Section VI.

V. COMPLEXITY ANALYSIS

In Section III and IV, we proposed the AO-based and SR-based transceiver design algorithms for problem (13) and (14), respectively. In this section, we compare the relative computational complexity of the proposed transceiver design algorithms. Moreover, we apply the same basic element of complexity analysis as in [42]. Among the proposed algorithms in this paper, we consider:

- *Non-robust AO*: the algorithm summarized in Table I.
- *Robust AO*: the algorithm summarized in Table II.
- *Non-robust SR*: the algorithm summarized in Table III.
- *Robust SR*: the algorithm summarized in Table IV.
- *Simplified non-robust SR*: the algorithm summarized in Table V.
- *Simplified robust SR*: the robust counterpart of the algorithm in Table V.

The complexity of the *non-robust AO* algorithm is dominated by solving problems (15) and (20) I_1 times, where I_1 denotes the iteration number. We note that the dual problems of (15) and (20) can be solved instead of (15) and (20) for better efficiency. Consider the dual problem of (15), which involves K LMI constraints of size N_t and on the order of $n_1 = \mathcal{O}(KN_t^2 + K)$ decision variables. Thus, the complexity of a generic interior-point method for solving problem (15) is given by $\mathcal{O}(n_1 \sqrt{KN_t} (KN_t^3 + n_1 KN_t^2 + n_1^2))$. Similarly, the complexity of solving the dual problem of (20) can be written as $\mathcal{O}(n_2 \sqrt{N_r^2} (N_r^6 + n_2 N_r^4 + n_2^2))$, where $n_2 = \mathcal{O}(N_r^4)$ is the order of the corresponding decision variables. The complexity of solving problem (65) can be neglected since it admits closed-form solution. Thus, the overall complexity of the *non-robust AO* algorithm is on the order of the quantity shown in the first row of Table VI.

The complexity of the *robust AO* algorithm is dominated by solving problems (26) and (31) I_2 times, plus the complexity of the rank-one recovery method. Problem (26) involves $KN_t^2 + 4K$ variables, $2K$ LMI constraints of size $N_r + 1$ and K LMI constraints of size N_t . Problem (31) involves $N_r^4 + 2K$ variables, $2K$ LMI constraints of size $N_r + 1$ and 1 LMI constraint of size N_r^2 . Moreover, the complexity of the rank-one recovery method in Table VII is dominated by

solving problem (64) R times, where R is the number of randomization steps.¹⁰ Problem (64) involves $2K$ variables and $2K$ second-order cone (SOC) constraints of dimension 3. Thus, the overall complexity of the *robust AO* algorithm is on the order of the quantity shown in the second row of Table VI.

The complexity of the *non-robust SR* algorithm is dominated by solving problem (49) BI_3 times, where I_3 is the iteration number, since the complexity of computing the affine approximation $\hat{x}_k(\mathbf{r}^{(i)}, \mathbf{r})$ and $\hat{z}_k(\mathbf{r}^{(i)}, \mathbf{r})$ is negligible compared to solving (49). Problem (49) involves $2K + 3$ SOC constraints, including 1 SOC of dimension $KN_t + 2$, 1 SOC of dimension $KN_r + 2$, K SOCs of dimension $K + 2$, and $K + 1$ SOCs of dimension 3. The number of variables is on the order of $\mathcal{O}(KN_t + 2K)$. It follows that the complexity of the *non-robust SR* algorithm is on the order of the quantity shown in the third row of Table VI.

The complexity of the *robust SR*, *simplified non-robust SR* and *simplified robust SR* algorithms can be analyzed in a similar way; the corresponding complexity figures are shown in the fourth to sixth rows of Table VI, respectively, where I_4 denotes the iteration number of the (*simplified*) *robust SR* algorithm. It is of interest to investigate the asymptotic complexity of the proposed algorithms when N_t , N_r and K are large, i.e., when we let $N_r = N_t = K \rightarrow \infty$. We further assume that $I_1 = I_2 = I_3 = I_4 = I$ for simplicity. Under these conditions, one can verify that the complexities of the proposed algorithms in Table VI are on the orders of $2IN_t^{13}$, $2\sqrt{3}IN_t^{13}$, $6BIN_t^{6.5}$, $3\sqrt{3}BIN_t^{10}$, $6(B+I)N_t^{6.5}$ and $3\sqrt{3}(B+I)N_t^{10}$, respectively. As seen, the robust algorithms always consume more computational resources than their non-robust counterparts, the SR-based algorithms have lower complexity compared with the AO-based algorithms and the simplified SR-based algorithms have the lowest complexity.

VI. SIMULATION RESULTS

In order to evaluate the performance of the proposed transceiver designs, numerical results have been obtained by performing computer simulations. In the simulations, we assume that both the first phase and the second phase channel coefficients are flat-fading i.i.d. with unit variance Rayleigh distribution. The nominal system configuration is defined by the following choice of parameters: $N_t = N_r = 4$, $K = 3$, $\xi = 1$, $\sigma_k^2 = \sigma^2 = -30\text{dBm}$, $\omega_k^2 = \omega^2 = -20\text{dBm}$, and $\sigma_r^2 = -30\text{dBm}$ unless otherwise specified. In addition, we assume equal SINR and EH thresholds at the destination receivers, i.e., $\gamma_k = \gamma$, $\psi_k = \psi$, $\forall k \in \mathcal{K}$, and equal norm bounds for the second phase channel error vectors, i.e., $\eta_{kj} = \eta$, $\forall j, k$ for simplicity. In the implementations of the various algorithms, the tolerance parameter is chosen as $\delta = 2 \times 10^{-3}$ while $I_1 = I_2 = 20$ and $I_3 = I_4 = 50$; all the rank-one recovery methods employ $R = 100$ randomization steps. All convex problems are solved by CVX [43] on a desktop Intel (i3-2100) CPU running at 3.1GHz with 4GB RAM.

¹⁰The complexity to recover \mathbf{W}^* is negligible since problem (65) has closed-form solution.

In the AO-based transceiver design algorithms, the RS AF matrices \mathbf{W} can be initialized in three different ways:

- *Init-1* : Initialize the RS AF matrix as an identity matrix.
- *Init-2* : Random matrices are generated according to normal distribution with zero mean and unit variance.
- *Init-3* : According to Section III and IV, the SR-based transceiver can be used to initialize the AO-based designs.

Fig. 3 shows the average power consumption performance versus the receiver EH target ψ for the AO-based transceiver designs with the three different initialization methods. From the results, we can see that the best performance is achieved by *Init-3* for both the non-robust and robust algorithms; *Init-1* and *Init-2* result into similar performance. For example, the power consumption of *Init-3* is 0.5dB less than that of *Init-1* and *Init-2* for the non-robust case, and the power saving rises up to 1dB for the robust case. As seen, the AO-based algorithms are sensitive to the initial point. The use of *Init-3* is not realistic in practice since it has to employ both the AO-based and the SR-based algorithms. However, in the following simulations, we employ *Init-3* as the initialization method for both the non-robust and robust AO algorithms, which serves as a performance bound unless otherwise stated.

Fig. 4 shows the performance comparison of the SR-based transceiver design algorithms proposed in Subsection IV-A and IV-B and the simplified SR-based transceiver design proposed in Subsection IV-C. It is worth noting that the algorithms with codebook size $B = 1$ only use the identity matrix as the permutation matrix (naive method)¹¹, and the algorithms with the $B = 8$ codebook employ the *Sum-Max* codebook design method. We include the identity matrix into the $B = 8$ codebook regardless of the singular values in order to guarantee that the performance of the algorithms with $B = 8$ is always better than with $B = 1$. We can see that the simplified SR-based transceiver design algorithms achieve almost the same performance as the non-simplified ones for both non-robust and robust cases. However, the simplified SR-based algorithms consume much less computational resources compared with their non-simplified counterparts. Thus, we employ the simplified SR-based design in the following simulations for comparison unless otherwise specified.

We compare the performance of the codebook design approaches, i.e., the *Sum-Max* and *Max-Min* methods, in terms of average power consumption. For completeness, we also consider the performance of a codebook whose elements (permutation matrices) are randomly selected. The results which are illustrated in Fig. 5 show the average power consumption performance curves versus EH target. We can see that the *Sum-Max* method outperforms other methods. Compared with the randomly generated codebook, the proposed *Sum-Max* method can lead to a power saving of 0.4dB for the non-robust case and 2dB for the robust case. The performance of the *Max-Min* method is slightly inferior to the *Sum-Max* method.

Fig. 6 shows the average power consumption performance for various codebook sizes in the SR-based transceiver design algorithms. It is observed that the SR-based robust transceiver

¹¹The naive method means that the RS only processes the received data vector \mathbf{y}_R by adjusting its power (i.e. scaling) and forwarding it.

TABLE VI
COMPLEXITY ANALYSIS OF THE PROPOSED TRANSCIVER DESIGNS

Proposed design	Complexity Order (suppressing the $\ln(1/\varepsilon)$)
Non-robust AO	$I_1(\mathcal{O}(n_1\sqrt{KN_t}(KN_t^3 + n_1KN_t^2 + n_1^2)) + \mathcal{O}(n_2N_r(N_r^6 + n_2N_r^4 + n_2^2)))$, $n_1 = \mathcal{O}(KN_t^2 + K)$, $n_2 = \mathcal{O}(N_r^4)$
Robust AO	$I_2(\mathcal{O}(n_1\sqrt{2K(N_r+1)} + KN_t(2K(N_r+1)^3 + KN_t^3 + 2n_1K(N_r+1)^2 + n_1KN_t^2 + n_1^2)) + \mathcal{O}(n_2\sqrt{2K(N_r+1)} + N_r^2(2K(N_r+1)^3 + N_r^6 + 2n_2K(N_r+1)^2 + n_2N_r^4 + n_2^2)) + R(\mathcal{O}(2K\sqrt{4K}(2K3^2 + 4K^2))))$, $n_1 = \mathcal{O}(KN_t^2 + 4K)$, $n_2 = \mathcal{O}(N_r^4 + 2K)$
Non-robust SR	$BI_3(\mathcal{O}(n\sqrt{4K} + 6((KN_t+2)^2 + (KN_r+2)^2 + K(K+2)^2 + (K+1)3^2 + n^2)))$, $n = \mathcal{O}(KN_t + 2K)$
Robust SR	$BI_4(\mathcal{O}(n_1\sqrt{2K(N_r+1)} + KN_t(2K(N_r+1)^3 + KN_t^3 + 2n_1K(N_r+1)^2 + n_1KN_t^2 + n_1^2)) + R(\mathcal{O}(2K\sqrt{4K}(2K3^2 + 4K^2))))$, $n_1 = \mathcal{O}(KN_t^2 + 4K)$.
Simplified non-robust SR	$(B + I_3)(\mathcal{O}(n\sqrt{4K} + 6((KN_t+2)^2 + (KN_r+2)^2 + K(K+2)^2 + (K+1)3^2 + n^2)))$, $n = \mathcal{O}(KN_t + 2K)$
Simplified robust SR	$(B + I_4)(\mathcal{O}(n_1\sqrt{2K(N_r+1)} + KN_t(2K(N_r+1)^3 + KN_t^3 + 2n_1K(N_r+1)^2 + n_1KN_t^2 + n_1^2)) + R(\mathcal{O}(2K\sqrt{4K}(2K3^2 + 4K^2))))$, $n_1 = \mathcal{O}(KN_t^2 + 4K)$.

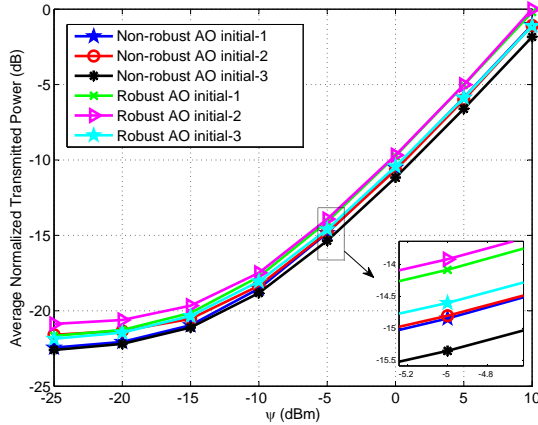


Fig. 3. Initialization methods comparison of the AO-based transceiver designs ($\eta = 0.1$, $\gamma = 10$ dB).

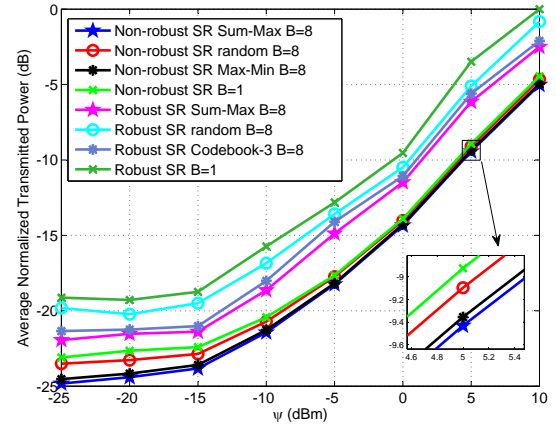


Fig. 5. Comparison of the codebook design methods for the SR-based transceiver designs ($\eta = 0.1$, $\gamma = 10$ dB, $\beta_i(0) = 1$, $\theta = 6$).

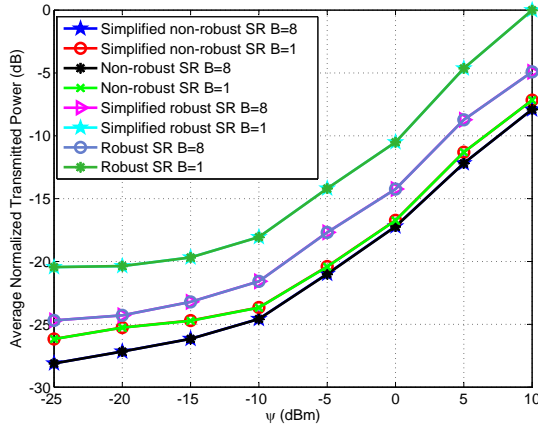


Fig. 4. Performance comparison of the non-simplified SR-based transceiver designs and the simplified SR-based transceiver designs ($\eta = 0.1$, $\gamma = 10$ dB, $\beta_i(0) = 1$, $\theta = 6$).

design algorithm with codebooks of size $B = 4, 8, 16$ and 24 achieves a power saving of 5dB compared to that with the $B = 1$ codebook, and its non-robust counterpart with codebooks of size $B = 4, 8, 16$ and 24 achieves about 1dB in power saving compared with the $B = 1$ codebook.¹² We can also see from

¹²Note that the algorithms with $B = 24$ codebook conduct a search for all the $N_r!$ permutation matrices, which is known as the optimal SR-based transceiver design algorithm.

this figure that an increase in B does not necessarily gives rise to an improvement of the power consumption performance when $B > 8$, which is the reason we proposed to construct a restricted number of transceivers, i.e., to select a small fraction of all the permutation matrices for transceiver design ($B \ll N_r!$).

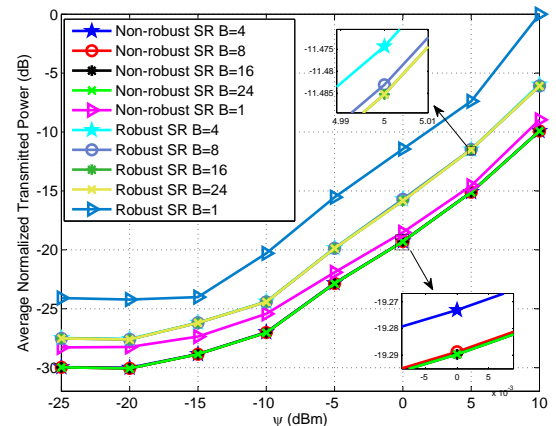


Fig. 6. Codebook size comparison of the SR-based transceiver designs ($\eta = 0.1$, $\gamma = 10$ dB, $\beta_i(0) = 1$, $\theta = 6$).

In the next series of simulations, we examine the comparative performance of the AO-based and SR-based transceiver design algorithms. Fig. 7 shows the average normalized trans-

mitted power versus ψ for these two algorithms. It is observed that the performance of the SR-based algorithms is very close to that of the AO-based algorithms. From the complexity analysis in Section VI, we note that if N_r increases, the complexity of solving problem (20) and (31) in the AO-based transceiver design might become unacceptable, which limits the practicality of the algorithm. Thus, the SR-based transceiver design is very promising and suitable for systems with large N_r . It is also important to mention that the number of signaling bits of the SR-based algorithms is much less than the AO-based algorithms since only the index of the optimal transceiver and the power scaling factor have to be sent to the RS instead of the whole RS AF matrix. Besides, a comparison of the feasibility rate between the AO-based and SR-based algorithms is provided. Specifically, Fig. 8 presents the feasibility rate comparison versus SINR target γ . One can observe that the feasibility rate performance of the AO-based algorithms is slightly inferior to that of the SR-based algorithms since we employ *Init-3* as the initialization method for the AO-based algorithms. Fig. 9 presents a similar comparison of the feasibility rate versus the channel error bound η . Similarly, from this figure, we can see that the performance of the AO-based algorithms and the SR-based algorithms is very close. The non-robust algorithms fail to satisfy both the SINR and EH constraints almost all the time under the NBE model.

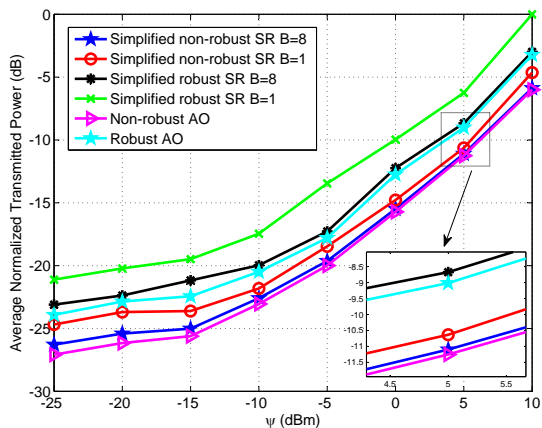


Fig. 7. Performance comparison of the SR-based transceiver designs and the AO-based transceiver designs ($\eta = 0.1$, $\gamma = 10$ dB, $\beta_l(0) = 1$, $\theta = 6$).

VII. CONCLUSION

In this paper, we considered the joint transceiver design problem for multiuser MISO relay systems with energy harvesting. We proposed AO-based and SR-based algorithms, including both non-robust and robust versions to CSI errors, for the joint optimization of the BS beamforming vectors, the RS AF matrix and the receiver PS ratios. Especially, the SR-based algorithms can achieve almost the same performance compared with the AO-based algorithms but with much reduced computational complexity and overhead. We also presented a simplified SR-based algorithm and carried out a detailed complexity analysis of all the proposed algorithms. Two efficient approaches for the design of the permutation

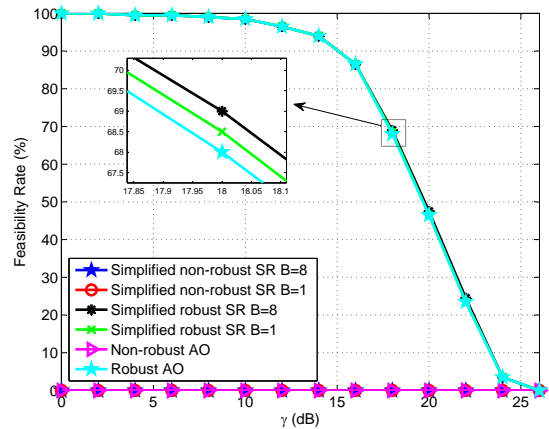


Fig. 8. Feasibility rate comparison of the SR-based transceiver designs and the AO-based transceiver designs versus SINR threshold γ ($\eta = 0.1$, $\beta_l(0) = 1$, $\theta = 6$).

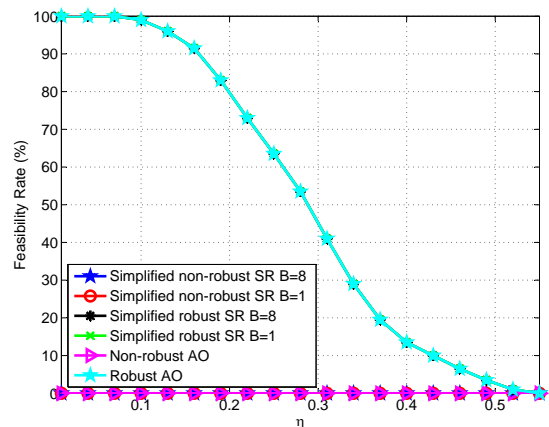


Fig. 9. Feasibility rate comparison of the SR-based transceiver designs and the AO-based transceiver designs versus CSI error bound η ($\gamma = 10$ dB, $\psi = 5$ dBm, $\beta_l(0) = 1$, $\theta = 6$).

matrix codebook in the SR-based algorithms were proposed. The simulation results validated the effectiveness of the proposed joint transceiver design algorithms and the necessity of using a robust formalism in the presence of imperfect CSI. We note that the proposed algorithms can be easily extended to more complicated (multi-hop) relay systems, which remains an open avenue for future work.

APPENDIX A

PROPOSED RANK-ONE RECOVERY METHOD

As we mentioned in Section III and IV, the optimal solution of problem (20), (26), (31) and (53) is not guaranteed to be rank-one. In this appendix, we propose a rank-one recovery method based on a randomization procedure. Inspired by the concept of worst-case robustness [44]–[46], we consider the following subproblems:

$$u_{kj} = \min_{\|\mathbf{e}_k\|^2 \leq \eta_k^2} |(\widehat{\mathbf{h}}_k^H + \mathbf{e}_k^H) \mathbf{W}^* \mathbf{G} \mathbf{f}_j^*|^2, \quad (59)$$

$$v_{kj} = \max_{\|\mathbf{e}_k\|^2 \leq \eta_k^2} |(\widehat{\mathbf{h}}_k^H + \mathbf{e}_k^H) \mathbf{W}^* \mathbf{G} \mathbf{f}_j^*|^2, \quad j \neq k, \quad (60)$$

$$\bar{w}_k = \max_{\|\mathbf{e}_k\|^2 \leq \eta_k^2} \|(\hat{\mathbf{h}}_k^H + \mathbf{e}_k^H)\mathbf{W}^*\|^2, \quad (61)$$

$$\tilde{w}_k = \min_{\|\mathbf{e}_k\|^2 \leq \eta_k^2} \|(\hat{\mathbf{h}}_k^H + \mathbf{e}_k^H)\mathbf{W}^*\|^2, \quad (62)$$

where \mathbf{f}_k^* and \mathbf{W}^* are extracted from the optimal solutions \mathbf{F}_k^* and \mathbf{W}^* using the randomization procedure as will be detailed in Table VII.¹³ It is not difficult to see that problem (59)-(62) can be solved by the Cauchy-Schwarz inequality and Lagrange multiplier method. We omit the detailed derivation and let $\{u_{kj}^*, v_{kj}^*, \bar{w}_k^*, \tilde{w}_k^*\}$ denote the corresponding optimal objective values.

For problem (26) and (53), we propose to scale up \mathbf{f}_k^* by $\sqrt{\varphi_k}$ and then jointly optimize $\{\sqrt{\varphi_k}\}$ and $\{\rho_k\}$ to recover a rank-one solution. The optimization problem can be formulated as

$$\begin{aligned} \min_{\{\varphi_k, \rho_k\}} & \sum_{k=1}^K \varphi_k \mathbf{f}_k^{*H} \mathbf{f}_k^* + \sum_{k=1}^K \varphi_k \|\mathbf{W}^* \mathbf{G} \mathbf{f}_k^*\|^2 \\ \text{s.t.} & \frac{\rho_k \varphi_k u_{kk}^*}{\rho_k \sum_{j \neq k} \varphi_j v_{kj}^* + \rho_k \sigma_r^2 \bar{w}_k^* + \rho_k \sigma_k^2 + \omega_k^2} \geq \gamma_k, \\ & \sum_{j=1}^K \varphi_j u_{kj}^* + \sigma_r^2 \tilde{w}_k^* + \sigma_k^2 \geq \frac{\psi_k}{\xi_k(1-\rho_k)}, \\ & \varphi_k \geq 0, 0 \leq \rho_k \leq 1, \forall k \in \mathcal{K}. \end{aligned} \quad (63)$$

The above problem can be reformulated as the following SOCP problem

$$\begin{aligned} \min_{\{\varphi_k, \rho_k\}} & \sum_{k=1}^K \varphi_k \mathbf{f}_k^{*H} \mathbf{f}_k^* + \sum_{k=1}^K \varphi_k \|\mathbf{W}^* \mathbf{G} \mathbf{f}_k^*\|^2 \\ \text{s.t.} & \|[2\omega_k, z_k - \rho_k]\| \leq z_k + \rho_k, \\ & \|[2\sqrt{\psi_k}/\xi_k, \tilde{z}_k - 1 + \rho_k]\| \leq \tilde{z}_k + 1 - \rho_k, \\ & z_k = \frac{\varphi_k u_{kk}^*}{\gamma_k} - \sum_{j \neq k} \varphi_j v_{kj}^* - \sigma_k^2 - \sigma_r^2 \bar{w}_k^*, \\ & \tilde{z}_k = \sum_{j=1}^K \varphi_j u_{kj}^* + \sigma_r^2 \tilde{w}_k^* + \sigma_k^2, \\ & \varphi_k \geq 0, 0 \leq \rho_k \leq 1, \forall k \in \mathcal{K}. \end{aligned} \quad (64)$$

Similarly, we also propose to scale up \mathbf{W}^* by $\sqrt{\varphi}$ and then jointly optimize $\{\sqrt{\varphi}\}$ and $\{\rho_k\}$ to recover a rank-one solution for problem (20) and (31). The optimization problem can be formulated as¹⁴

$$\begin{aligned} \min_{\{\varphi, \rho_k\}} & \sum_{k=1}^K \varphi \|\mathbf{W}^* \mathbf{G} \mathbf{f}_k^*\|^2 + \sigma_r^2 \varphi \|\mathbf{W}^*\|^2 \\ \text{s.t.} & \frac{\rho_k \varphi u_{kk}^*}{\rho_k \varphi \sum_{j \neq k} v_{kj}^* + \varphi \rho_k \sigma_r^2 \bar{w}_k^* + \rho_k \sigma_k^2 + \omega_k^2} \geq \gamma_k, \\ & \varphi \sum_{j=1}^K u_{kj}^* + \varphi \sigma_r^2 \tilde{w}_k^* + \sigma_k^2 \geq \frac{\psi_k}{\xi_k(1-\rho_k)}, \\ & \varphi \geq 0, 0 \leq \rho_k \leq 1, \forall k \in \mathcal{K}. \end{aligned} \quad (65)$$

As has been discussed in our previous work [47], the above optimization problem admits a closed-form solution and we omit the detailed derivation in this work. The proposed rank-one recovery method is summarized in Table VII.¹⁵

¹³For problem (53), \mathbf{W}^* can be expressed as $\sqrt{\beta_l^*} \mathbf{T}_l$, where β_l^* denotes the relay power scaling factor corresponding to the l th latent transceiver.

¹⁴For problem (20), $\{u_{kj}^*, v_{kj}^*, \bar{w}_k^*, \tilde{w}_k^*\}$ is the solution of (59)-(62) with $\mathbf{e}_k = \mathbf{0}$, $\forall k$.

¹⁵We only list the detailed steps to recover \mathbf{f}_k^* , which can be easily extended to the recovery of \mathbf{W}^* .

TABLE VII
PROPOSED RANK-ONE RECOVERY METHOD

1. For the i th randomization step ($i = 1, \dots, R$, R is the number of randomization steps.)
 2. - If $i = 1$, let \mathbf{f}_k^* equal to the principal component of \mathbf{F}_k^* . Else, calculate the eigenvalue decomposition $\mathbf{F}_k^* = \mathbf{Q} \mathbf{\Lambda} \mathbf{Q}^H$, then the candidate vector is generated as $\mathbf{f}_k^* = \mathbf{Q} \mathbf{\Lambda}^{\frac{1}{2}} \mathbf{w}$, where \mathbf{w} is an i.i.d. complex Gaussian vector with zero mean and unit variance.
 - Solve problem (64) to obtain the optimal $\{\varphi_k^*, \rho_k^*\}$. If the problem turns out to be infeasible, discard that candidate vector. Otherwise, save the candidate $\{\mathbf{f}_k^*, \varphi_k^*, \rho_k^*\}$ and the objective value of the problem.
- End**
4. Select the candidate $\{\mathbf{f}_k^*, \varphi_k^*, \rho_k^*\}$ which corresponds to the minimum objective value.

APPENDIX B

THE PROOF OF PROPOSITION 1

We first introduce four sets of auxiliary variables d_k, \tilde{d}_k, e_k and $\tilde{e}_k, \forall k \in \mathcal{K}$, which satisfy

$$d_k = \sigma_r^2 \mathbf{h}_k^H \mathbf{h}_k + \frac{1}{4} \omega_k^2 (p_k - \varphi_l^{(i)})^2 + \frac{1}{\gamma_k} \mathbf{f}_k^{(i)H} \tilde{\mathbf{G}}_k \mathbf{f}_k^{(i)}, \quad (66)$$

$$\tilde{d}_k = -\sigma_k^2 \varphi_l + \frac{1}{2} (p_k - \varphi_l^{(i)}) (p_k - \varphi_l) + \frac{2}{\gamma_k} \mathcal{R}\{\mathbf{f}_k^{(i)H} \tilde{\mathbf{G}}_k \mathbf{f}_k^{(i)}\}, \quad (67)$$

$$e_k = -\sigma_r^2 \mathbf{h}_k^H \mathbf{h}_k + \sum_{j=1}^K \mathbf{f}_j^{(i)H} \tilde{\mathbf{G}}_k \mathbf{f}_j^{(i)} + \frac{\psi_k}{4\xi_k} (q_k^{(i)} - \varphi_l^{(i)})^2, \quad (68)$$

$$\tilde{e}_k = 2\mathcal{R}\left\{\sum_{j=1}^K \mathbf{f}_j^{(i)H} \tilde{\mathbf{G}}_k \mathbf{f}_j^{(i)}\right\} + \frac{\psi_k}{2\xi_k} (q_k^{(i)} - \varphi_l^{(i)}) (q_k - \varphi_l) + \sigma_k^2 \varphi_l, \quad (69)$$

where d_k and e_k are constant scalars while \tilde{d}_k and \tilde{e}_k are affine functions in \mathbf{r} . Then, the SINR constraints in problem (48) can be rewritten as the following SOCs

$$\left\| \left[\mathbf{w}_k^T, \frac{\tilde{d}_k - d_k - 1}{2} \right] \right\| \leq \frac{\tilde{d}_k - d_k + 1}{2}, \forall k, \quad (70)$$

where

$$\mathbf{w}_k = [\mathbf{h}_k^H \mathbf{T}_l \mathbf{G} \mathbf{f}_1, \dots, \mathbf{h}_k^H \mathbf{T}_l \mathbf{G} \mathbf{f}_{k-1}, \mathbf{h}_k^H \mathbf{T}_l \mathbf{G} \mathbf{f}_{k+1}, \dots, \mathbf{h}_k^H \mathbf{T}_l \mathbf{G} \mathbf{f}_K, \frac{1}{2} \omega_k (p_k + \varphi_l)]^T. \quad (71)$$

Similarly, the EH constraints in problem (48) can be reformulated as the following SOCs

$$\left\| \left[\sqrt{\frac{\psi_k}{4\xi_k}} (q_k + \varphi_l), \frac{\tilde{e}_k - e_k - 1}{2} \right] \right\| \leq \frac{\tilde{e}_k - e_k + 1}{2}, \forall k. \quad (72)$$

Next, by introducing slack variables P_1, P_2 and P_3 , we can equivalently write the objective function $P_l(\mathbf{r})$ of problem (48) as follows

$$P_l(\mathbf{r}) = P_1 + P_2 + P_3, \quad (73)$$

where

$$\|[\mathbf{f}_1^T, \dots, \mathbf{f}_K^T, (P_1 - 1)/2]\| \leq (P_1 + 1)/2, \quad (74)$$

$$\|[(\mathbf{G} \mathbf{f}_1)^T, \dots, (\mathbf{G} \mathbf{f}_K)^T, (P_2 - \varphi_l)/2]\| \leq (P_2 + \varphi_l)/2, \quad (75)$$

$$\| [2\sigma_r, \varphi_l - P_3] \| \leq \varphi_l + P_3. \quad (76)$$

Therefore, problem (48) can be shown to be equivalent to the following SOCP problem

$$\begin{aligned} & \min_{r, P_1, P_2, P_3} P_1 + P_2 + P_3 \\ & \text{s.t. (70), (72), (74), (75) and (76),} \\ & p_k \geq 1, q_k \geq 1, \text{invp}(p_k) + \text{invp}(q_k) \leq 1, \forall k \in \mathcal{K}. \end{aligned} \quad (77)$$

This completes the proof.

REFERENCES

- [1] L. R. Varshney, "Transporting information and energy simultaneously," in *IEEE Int. Symp. Inf. Theory (ISIT)*, pp. 1612–1616, Jul. 2008.
- [2] P. Grover and A. Sahai, "Shannon meets Tesla: Wireless information and power transfer," in *IEEE Int. Symp. Inf. Theory (ISIT)*, pp. 2363–2367, Jun. 2010.
- [3] P. Popovski, and O. Simeone, "Two-way communication with energy exchange," in *Proc. IEEE Inf. Theory Workshop*, pp. 592–596, Sept. 2012.
- [4] A. Fouladgar and O. Simeone, "On the transfer of information and energy in multi-user systems," *IEEE Commun. Lett.*, vol. 16, no. 11, pp. 1733–1736, Nov. 2012.
- [5] R. Zhang and C. K. Ho, "MIMO broadcasting for simultaneous wireless information and power transfer," *IEEE Trans. Wireless Commun.*, vol. 12, no. 5, pp. 1989–2001, May 2013.
- [6] L. Liu, R. Zhang, and K.-C. Chua, "Wireless information and power transfer: A dynamic power splitting approach," *IEEE Trans. Commun.*, vol. 61, no. 9, pp. 3990–4001, Sept. 2013.
- [7] X. Zhou, R. Zhang, and C. K. Ho, "Wireless information and power transfer: Architecture design and rate-energy tradeoff," *IEEE Trans. Commun.*, vol. 61, no. 11, pp. 4754–4767, Nov. 2013.
- [8] Q. Shi, W. Xu, L. Liu and R. Zhang, "Joint transmit beamforming and receive power splitting for MISO SWIPT systems," *IEEE Trans. Wireless Commun.*, vol. 13, no. 6, pp. 3269–3280, Jun. 2014.
- [9] S. Timotheou, I. Krikidis, G. Zheng and B. Ottersten, "Beamforming for MISO interference channels with QoS and RF energy transfer," *IEEE Trans. Wireless Commun.*, vol. 13, no. 5, pp. 2646–2658, May 2014.
- [10] Q. Shi, W. Xu, T.-H. Chang, Y. Wang, and E. Song, "Joint beamforming and power splitting for MISO interference channel with SWIPT: An SOCP relaxation and decentralized algorithm," *IEEE Trans. Signal Process.*, vol. 62, no. 23, pp. 6194–6208, Dec. 2014.
- [11] B. Chalise, Y. Zhang, and M. Amin, "Energy harvesting in an OSTBC based amplify-and-forward MIMO relay system," in *Proc. IEEE Int. Conf. on Acoustics, Speech and Signal Processing*, pp. 3201–3204, Mar. 2012.
- [12] Q. Li, Q. Zhang, and J. Qin, "Beamforming in non-regenerative two-way multi-antenna relay networks for simultaneous wireless information and power transfer," *IEEE Trans. Wireless Commun.*, vol. 13, no. 10, pp. 5509–5520, Oct. 2014.
- [13] G. Li, P. Ren, G. Lv, and Q. Du, "High-rate relay beamforming for simultaneous wireless information and power transfer," *Electronics Letters*, vol. 50, no. 23, pp. 1759–1761, 2014.
- [14] H. Chen, Y. Li, Y. Jiang, Y. Ma, and B. Vucetic, "Distributed power splitting for SWIPT in relay interference channels using game theory," *IEEE Trans. Wireless Commun.*, vol. 14, no. 1, pp. 410–420, Jan. 2015.
- [15] T. Tang, C. B. Chae, R. W. Heath, and S. Y. Cho, "On achievable sum rates of a multiuser MIMO relay channel," in *IEEE Int. Symp. Inf. Theory (ISIT)*, pp. 1026–1030, Jul. 2006.
- [16] K. S. Gomadam and S. A. Jafar, "On the duality of MIMO MAC and BC with AF relays," in *Proc. IEEE Asilomar Conf. Signals, Syst. Comput.*, pp. 863–867, Nov. 2007.
- [17] R. Zhang, C. C. Chai, and Y.-C. Liang, "Joint beamforming and power control for multi-antenna relay broadcast channel with QoS constraints," *IEEE Trans. Signal Process.*, vol. 57, no. 2, pp. 726–737, Feb. 2009.
- [18] D. Feng, C. Jiang, G. Lim, L. J. Cimini, Jr., G. Feng, and G. Y. Li, "A survey of energy-efficient wireless communications," *IEEE Commun. Surveys Tutorials*, vol. 15, no. 1, pp. 167–178, First Quarter 2013.
- [19] G. Y. Li, Z. Xu, C. Xiong, C. Yang, S. Zhang, Y. Chen, and S. Xu, "Energy-efficient wireless communications: tutorial, survey, and open issues," *IEEE Wireless Commun.*, pp. 28–35, Dec. 2011.
- [20] N. Banerjee, M. D. Corner, D. Towsley, and B. N. Levine, "Relays, base stations, and meshes: enhancing mobile networks with infrastructure," in *Proc. MOBICOM*, San Francisco, USA., pp. 81–91, Sep. 2008.
- [21] Z.-Q. Luo, W.-K. Ma, A.-C. So, Y. Ye, and S. Zhang, "Semidefinite relaxation of quadratic optimization problems," *IEEE Trans. Signal Process. Mag.*, vol. 27, no. 3, pp. 20–34, May 2010.
- [22] S. Boyd and L. Vandenberghe, *Convex Optimization*. Cambridge, U.K.: Cambridge Univ. Press, 2004.
- [23] S. P. Boyd, L. El Ghaoui, E. Feron, and V. Balakrishnan, *Linear Matrix Inequalities in System and Control Theory*. SIAM, vol. 15, 1994.
- [24] Y. Cai, R. de Lamare, L. Yang and M. Zhao, "Robust MMSE precoding based on switched relaying and side information for multiuser MIMO relay systems," to appear in *IEEE Trans. Veh. Technol.*
- [25] A. L. Yuille and A. Rangarajan, "The concave-convex procedure," *Neural Computation*, vol. 15, no. 4, pp. 915–936, 2003.
- [26] G. R. Lanckriet and B. K. Sriperumbudur, "On the convergence of the concave-convex procedure," in *Advances in Neural Information Processing Systems*, pp. 1759–1767, 2009.
- [27] J. N. Laneman, G. W. Wornell, and D. N. C. Tse, "An efficient protocol for realizing cooperative diversity in wireless networks," in *IEEE Int. Symp. Inf. Theory (ISIT)*, pp. 294, Jun. 2001.
- [28] T. Kong and Y. Hua, "Optimal design of source and relay pilots for MIMO relay channel estimation," *IEEE Trans. Signal Process.*, vol. 59, no. 9, pp. 4438–4446, Sept. 2011.
- [29] S. Sun and Y. Jing, "Channel training design in amplify-and-forward MIMO relay networks," *IEEE Trans. Wireless Commun.*, vol. 10, no. 10, pp. 3380–3391, Oct. 2011.
- [30] F.-S. Tseng, W.-J. Huang, and W.-R. Wu, "Robust far-end channel estimation in three-node amplify-and-forward MIMO relay systems," *IEEE Trans. Veh. Technol.*, vol. 62, no. 8, pp. 3752–3766, Oct. 2013.
- [31] F. W. Vook, X. Zhuang, K. L. Baum, T. A. Thomas, and M. C. Cudak, "Signaling methodologies to support closed-loop transmit processing in TDD-OFDMA," *IEEE C802.16e-04/103r2*, Jul. 2004.
- [32] C. Chae, D. Mazzaresse, T. Inoue, and R. W. Heath, Jr., "Coordinated beamforming for the multiuser MIMO broadcast channel with limited feedforward," *IEEE Trans. Signal Process.*, vol. 56, no. 12, pp. 6044–6056, Dec. 2008.
- [33] Y. Cai, R. C. de Lamare, and R. Fa, "Switched interleaving techniques with limited feedback for interference mitigation in DS-SSMA systems," *IEEE Trans. Commun.*, vol. 59, no. 7, pp. 1946–1956, Jul. 2011.
- [34] P. Ubaidulla and A. Chockalingam, "Relay precoder optimization in MIMO-relay networks with imperfect CSI," *IEEE Trans. Signal Process.*, vol. 59, no. 11, pp. 5473–5484, Nov. 2011.
- [35] M. Biguesh, S. Shahbazpanahi, and A. B. Gershman, "Robust downlink power control in wireless cellular systems," *EURASIP J. Wireless Commun. Netw.*, vol. 2, pp. 261–272, 2004.
- [36] Q. Shi, W. Xu, L. Liu and R. Zhang, "Joint transmit beamforming and receive power splitting for MISO SWIPT systems," *IEEE Trans. Wireless Commun.*, vol. 13, no. 6, pp. 3269–3280, Jun. 2014.
- [37] R. H. Tütüncü, K. C. Toh and M. J. Todd, "Solving semidefinite-quadratic-linear programs using SDPT3," *Math. Program., Ser. B*, vol. 95, no. 2, pp. 189–217, 2003.
- [38] D. H. Brandwood, "A complex gradient operator and its application in adaptive array theory," in *Proc. Inst. Elect. Eng.*, vol. 130, no. 1, pp. 11–16, 1983.
- [39] Y. Cheng and M. Pesavento, "Joint optimization of source power allocation and distributed relay beamforming in multiuser peer-to-peer relay networks," *IEEE Trans. Signal Process.*, vol. 60, no. 6, pp. 2962–2973, Jun. 2012.
- [40] G. Zheng, S. Chatzinotas, and B. Ottersten, "Generic optimization of linear precoding in multibeam satellite systems," *IEEE Trans. Wireless Commun.*, vol. 11, no. 6, pp. 2308–2320, Jun. 2012.
- [41] H. Pennanen, A. Tölli, and M. Latva-aho, "Decentralized robust beamforming for coordinated multi-Cell MISO networks," *IEEE Signal Processing Letters*, vol. 21, no. 3, pp. 334–338, Mar. 2014.
- [42] K.-Y. Wang, A. Man-Cho So, T.-H. Chang, W.-K. Ma, and C.-Y. Chi, "Outage constrained robust transmit optimization for multiuser MISO downlinks: tractable approximations by conic optimization," *IEEE Trans. Signal Process.*, vol. 62, no. 21, pp. 5690–5705, Nov. 2014.
- [43] C. R. Inc., "Cvx: Matlab software for disciplined convex programming," Available: <http://cvxr.com/cvx>, Sept. 2012.
- [44] J. Li, P. Stoica, and Z. Wang, "On robust capon beamforming and diagonal loading," *IEEE Trans. Signal Process.*, vol. 51, no. 7, pp. 1702–1715, Jul. 2003.
- [45] —, "Doubly constrained robust capon beamformer," *IEEE Trans. Signal Process.*, vol. 52, no. 9, pp. 2407–2423, Sept. 2004.
- [46] S.-J. Kim, A. Magnani, A. Mutapcic, S. P. Boyd, and Z.-Q. Luo, "Robust beamforming via worst-case SINR maximization," *IEEE Trans. Signal Process.*, vol. 56, no. 4, pp. 1539–1547, Apr. 2008.

- [47] M. M. Zhao, Y. Cai, Q. Shi, B. Champagne and M. J. Zhao , “Robust transceiver design for MISO interference channel with energy harvesting,” submitted for publication, available on-line at arXiv : 1501.07658.